and testosterone levels in rat testes [15]. Recently reported adverse effects of BPA on in situ steroidogenesis include increased testosterone levels in mouse Leydig cells and decreased E_2 levels in porcine ovarian granulosa cells [16, 17]. Thus, BPA may have the potential not only to mimic estrogenic action but also to alter in situ steroidogenesis in the prostate as well as other reproductive organs.

To investigate the effects of fetal exposure to low-dose BPA on in situ steroidogenesis in the developing prostate, we first measured sex steroid hormone levels and CYP19A1 (aromatase) activity in the BPA-treated mouse urogenital sinus (UGS), from which the prostate develops embryologically. Subsequently, we examined the alterations of steroidogenic enzyme gene expression to confirm the alterations of the in situ sex steroid hormonal environment in the BPA-treated mouse UGS. Finally, we identified the BPA-specific biological effects for in situ steroidogenesis during fetal prostate development.

MATERIALS AND METHODS

Animals

In the present study, 36 pregnant female C57BL/6 mice were purchased on the 12th day of gestation from Japan SLC, where the breeding strategy was to mate three female C57BL/6 mice (age, 10 wk) with one male overnight and separate them the next morning (plug date denoted as Day 0). All animals were housed individually in chip-bedded polyolefin cages in a room with controlled temperature (23 ± 1°C) and humidity (45 to 65%) on a 12L:12D photoperiod. Mice were fed a low-phytoestrogen diet (NIH-07PLD; Oriental Yeast Co.) and tap water ad libitum.

Chemicals

For the present study, both BPA and DES with a purity of 99% or greater were purchased from Nacalai Tesque and Wako Pure Chemical Industries, respectively.

Fetal Exposure to Chemicals

We randomly assigned 36 pregnant female C57BL/6 mice to three different treatment groups: BPA (20 $\mu g\ kg^{-1}\ day^{-1}$, n = 12) or DES (0.2 $\mu g\ kg^{-1}\ day^{-1}$, n = 12), both of which were dissolved in tocopherol-stripped corn oil (MP Biomedical, Inc.), administered by oral gavages on Embryonic Day (E) 13 to E16 and the control group, in which pregnant mice were fed tocopherol-stripped corn oil (2 ml/kg, n = 12). Previously, our group reported that this protocol of fetal exposure to BPA and DES resulted in similar histopathological changes of adult prostate—that is, increased basal epithelial cell number and induction of cytokeratin 10, a classic marker associated with squamous differentiation, in such cells [8]. Our dose level of BPA for the present study was also based on reported results suggesting that BPA is less than 100-fold less potent than DES. The Mie University's Committee on Animal Investigation approved the experimental protocol.

Termination and UGS Dissection

Between E17 and Postnatal Day (P) 1, all animals were terminated by an overdose of isoflurane followed by cervical dislocation. For each of the three groups, from 15 to 18 fetuses (both male and female) from three pregnant mice were collected at E17, E18, P0, and P1. The bladder and urethra were removed and dissected to isolate the UGS, and then the five or six UGS obtained were pooled as one sample. Thus, the 15–18 UGS were divided into three samples at each time point. The UGS, cerebellum, heart, kidney, testis, and ovary were collected in RNAlater (Applied Biosystems).

To isolate pure UGS, other tissues, such as the bladder, urethra, wolffian duct, seminal vesicle, and mullerian duct, were removed from both the male and female urogenital tracts. The histopathology of the mouse UGS was then examined by hematoxylin-and-eosin staining.

Measurements of In Situ E_2 Levels and CYP19A1 (Aromatase) Activity in UGS

The E_2 levels and CYP19A1 (aromatase) activity in UGS were determined by liquid chromatography-tandem mass spectrometry [18] and a tritiated water release assay [19], respectively, which were made available by Aska Pharma Medical. Briefly, the organs were homogenized, and the extracts were applied to a C18 Amprep solid-phase column (Amersham Biosciences) to remove contaminating fats. The E_2 was then separated using a normal-phase high-performance liquid chromatography system (Jasco) with a silica gel column (Cosmosil 5SI; Nacalai Tesque), and 100 pg of isotope-labeled $[^{13}C_4]E_2$ were added to extracts. The evaporated extracts were reacted with 5% pentafluorobenzyl bromide/acetonitrile, under KOH/ethanol, for 1 h at 55°C. After evaporation, the products were reacted with 100 ml of picolinic acid solution (2% picolinic acid, 2% 2-dimethylaminopyridinc, and 1% 2-methyl-6-nitrobenzoic acid in tetrahydrofuran) and 20 ml of triethylamine for 0.5 h at room temperature. The reaction products were dissolved in 1% acetic acid and then purified using a Bond Elute C18 column (Varian). The products were measured with a reverse-phase liquid chromatograph (Agilent 1100; Agilent Technologies) coupled with an API 5000 triple-stage quadrupole mass spectrometer (Applied Biosystems) in the positive-ion mode. This device monitored the *m/z* 558 to *m/z* 339 (E_2) and *m/z* 562 to *m/z* 343 ($[^{13}C_4]E_2$) transitions.

The tritiated water release assay was used for the measurement of CYP19A1 (aromatase) activity. This method measures the production of ^3H_2O, which forms as a result of aromatization of the substrate [1b-^{3}H]androst-4-ene-3,17-dione (New England Nuclear). Serum-free medium containing [1b-^{3}H]androst-4-ene-3,17-dione solution (54 nM) was prepared, of which 0.5 ml was added to each sample. After incubation for 1 h, the samples were placed on ice, and 200 μl of culture medium were withdrawn. The medium was extracted with 500 μl of chloroform, vortexed, and then centrifuged for 1 min at 9000 × *g*. A 100-μl aliquot of the aqueous phase was mixed with 100 μl of a 5% (wt/vol) charcoal/0.5% (wt/vol) dextran T-70 suspension, vortexed, and then incubated at room temperature for 10 min. Then, after centrifugation of the solution for 5 min at 9000 × *g*, a 150-μl aliquot was removed for measurement of radioactivity by liquid scintillation.

RNA Extraction and cDNA Preparation

Total RNA was extracted using the RNeasy Mini Kit (Qiagen, Inc.) in accordance with the manufacturer's instructions. The RNA concentration was then determined spectrophotometrically by a multidetection microplate reader (Dainippon Sumitomo Pharma Co.). From 50 ng of total RNA, cDNA was reverse transcribed using oligo(dT) and Superscript II RNase H-reverse transcriptase (Invitrogen) as previously described [8].

Analysis of Gene Expression Profile

For determining gene expression profiles of the male UGS, GeneChip analysis with the Percellome method was performed [20]. Briefly, organs were prepared using RLT buffer (Qiagen, Inc.). Total RNA was extracted using RNeasy Mini Kit. First-strand cDNA was synthesized by incubating 5 mg of total RNA with a T7 oligo(dT) primer (Invitrogen) according to the manufacturer's protocol. The dsDNA was mixed with T7 RNA polymerase (Enzo Biochem, Inc.). During the in vitro transcription, generated cRNAs were labeled with biotin-16-UTP and biotin-11-CTP (Enzo Biochem, Inc.). The purified cRNA was fragmented at 300–500 bp into the target solution. Hybridization was performed with the GeneChip Mouse Genome 430 Version 2.0 (Affymetrix, Inc.) at 45°C for 18 h after staining with streptavidin-R-phycoerythrin conjugates (Molecular Probes, Invitrogen). The reacted arrays were then scanned as digital image files, and the scanned data were analyzed with GeneChip Operating Software (Affymetrix, Inc.). The expression data were converted to copy numbers of mRNA per cell by the Percellome method, quality controlled, and analyzed using Percellome software [20].

Real-Time PCR Analysis

Real-time PCR was carried out in the iCycler iQ Detection System (Bio-Rad Laboratories) with iQ SYBR-Green Supermix reagents (Bio-Rad Laboratories) as previously described [8]. The PCR amplification reaction was performed with specific primers as shown in Table 1. After PCR, melting-curve analysis was performed to verify specificity and identity of the PCR products. All data were analyzed with the iCycler iQ Optical System Software Version 3.0A (Bio-Rad Laboratories). All PCR data were normalized to *Gapdh* mRNA.

Preparation of Primary Cultured Mesenchymal Cells from UGS

The UGS were dissected from the fetuses and separated into UGE and urogenital sinus mesenchyme (UGM) by tryptic digestion and mechanical separation as previously described [21]. UGM were cultured in RPMI-1640

TABLE 1. Sequences of oligonucleotide primers used for the real-time PCR analyses.

Gene	Primer[a]
Capdh	F: 5′-AAATGGTGAAGGTCGGTGTG-3′
	R: 5′-TGAAGGGGTCGTTGATGG-3′
Cyp19a1	F: 5′-GCCCAATGAATTTACCCTCGAA-3′
	R: 5′-AAGCCAAAAGGCTGAAAGTACCT-3′
Cyp11a1	F: 5′-TCGACTCCTCAGAACTAAGACCTG-3′
	R: 5′-GTACCCTGGTGTCCTTTATAGCCT-3′
Nr5a1	F: 5′-CCTGGGCTGGCTACCTCTATC-3′
	R: 5′-CGAACTAGAGCCAGAGGAGGAC-3′
Esr1	F: 5′-GCACAGGATGCTAGCCTTGTCTC-3′
	R: 5′-AATTGTCACCAGCTTGCAGGTTC-3′
Ar	F: 5′-GGCGGTCCTTCACTAATGTCAACT-3′
	R: 5′-CTGACTTGTGCATGCGGTACTCAT-3′
Esrrg	F: 5′-CCGAGAGTTGGTGGTTATCATTGG-3′
	R: 5′-GGAAGACCCTCGCCGTGC-3′

[a] F, forward; R, reverse.

with 5% fetal bovine serum and plated out on four-well glass slides (BD Falcon). After several days, cells were fixed in methanol and processed for immunocytochemical analysis.

Immunocytochemical Staining

The sections were first incubated for 15 min in 0.01 M PBS. After inhibition of endogenous peroxidases (10 min in 0.6% H_2O_2 diluted in 0.01 M PBS plus 0.2% Triton X-100 [PBST]) and saturation (2 h in a 5% normal goat serum solution), sections were incubated overnight at 4°C in a polyclonal affinity-purified antiaromatase antibody or estrogen-related receptor gamma (ESRRG) antibody raised in rabbit against quail recombinant aromatase or ESRRG diluted 1:500 in 0.01 M PBST. The next day, the sections were immersed for 2 h at room temperature in a biotin-conjugated goat anti-rabbit immunoglobulin G (DakoCytomation, Inc.) diluted 1:400 in PBST and then for 2 h in a streptavidin-fluorescein complex (Rhodamine; DakoCytomation, Inc.) diluted 1:50 in PBST. Between each step, sections were extensively rinsed in PBST. The sections were mounted onto microscope slides, coverslipped with a gelatin-based mounting medium, and stored in the dark at 4°C. For double-labeling immunofluorescence, Alexa Fluor 488- or 594-conjugated secondary antibodies were used. Rabbit polyclonal anti-aromatase antibody was kindly provided by Prof. Nobuhiro Harada (Department of Biochemistry, Fujita Health University School of Medicine, Aichi, Japan) [22]. The rabbit polyclonal anti-ESRRG antibody used in the present study was established and characterized as previously reported [23]. The mouse monoclonal anti-Ran antibody (Santa Cruz Biotechnology, Inc.) was used to detect nucleus in cells. Ran, also called TC4, is the small RAS-related protein that is localized in the nucleus.

Statistical Analysis

Results are expressed as the mean ± SD. Differences among the three groups were determined using Student *t*-test with Dunnett multiple comparison. A value of $P < 0.05$ was considered to be statistically significant.

RESULTS

BPA-Specific Increases of E_2 Levels and CYP19A1 (Aromatase) Activity in Mouse UGS

The pregnant mice were exposed to low-dose BPA during the onset of prostatic budding (E13–E16), and the UGS of fetuses were collected during bud elongation (E17–P1). In analyses of in situ sex steroid hormonal environment, E_2 levels and CYP19A1 (aromatase) activity were significantly increased only at P1 in BPA-treated UGS, not at P1 in the DES-treated UGS (Fig. 1). At E17 and P1, both the E_2 levels and CYP19A1 (aromatase) activity in untreated male UGS were not significantly different compared with those in untreated female UGS.

BPA-Specific Up-Regulation of Steroidogenic Enzyme and Sex-Determining Gene mRNA in Mouse UGS

To investigate the BPA-specific gene alterations related to increases of the E_2 levels and aromatase activity, we performed preliminary GeneChip analysis with the Percellome method in the BPA- or DES-treated male UGS at E17 and P1. The results showed BPA-specific mRNA up-regulation of steroidogenic enzymes, such as *Cyp11a1*, *Cyp11b1*, and *Cyp17a1*, and sex-determining factors, such as *Nr5a1*, *Nr0b1*, *Gata4*, and *Amhr2* (data not shown). Furthermore, quantitative PCR analysis confirmed the mRNA up-regulation of *Cyp19a1*, *Cyp11a1*, and *Nr5a1* only in the BPA-treated neonatal (P0 and P1) UGS, not in the DES-treated neonatal UGS (Fig. 2). No difference in mRNA expression levels was found between E17 and P1 when comparing the untreated male UGS to that of the female. In

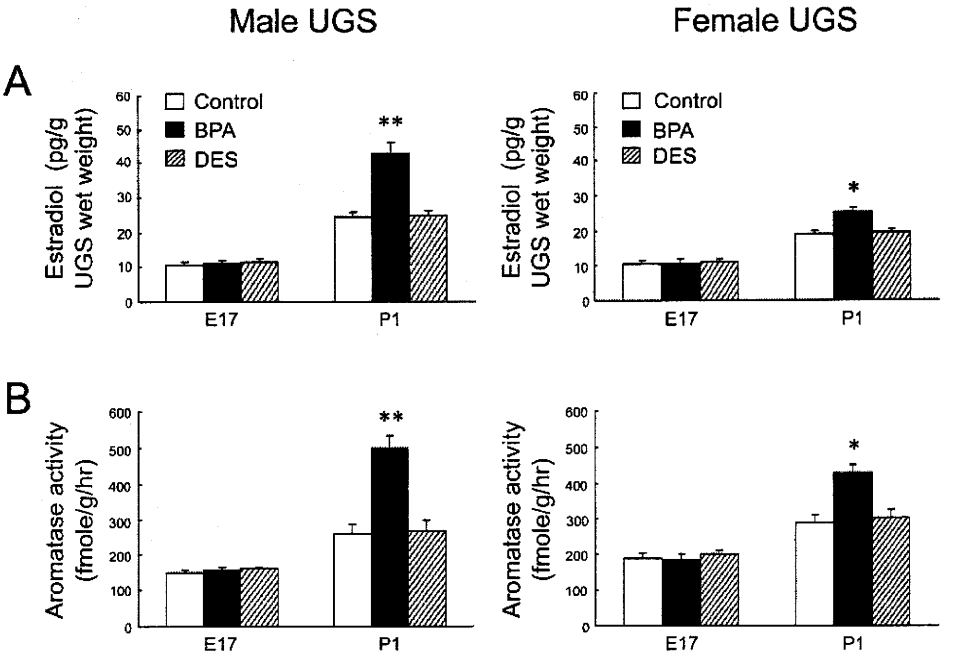

FIG. 1. BPA-specific increases of E_2 levels and CYP19A1 (aromatase) activity in mouse UGS. E_2 levels (**A**) and CYP19A1 (aromatase) activity (**B**) were measured in the untreated control (open bar), BPA-treated UGS (closed bar), and DES-treated UGS (slashed bar) at E17 and P1. $*P < 0.01$, $**P < 0.001$ vs. control.

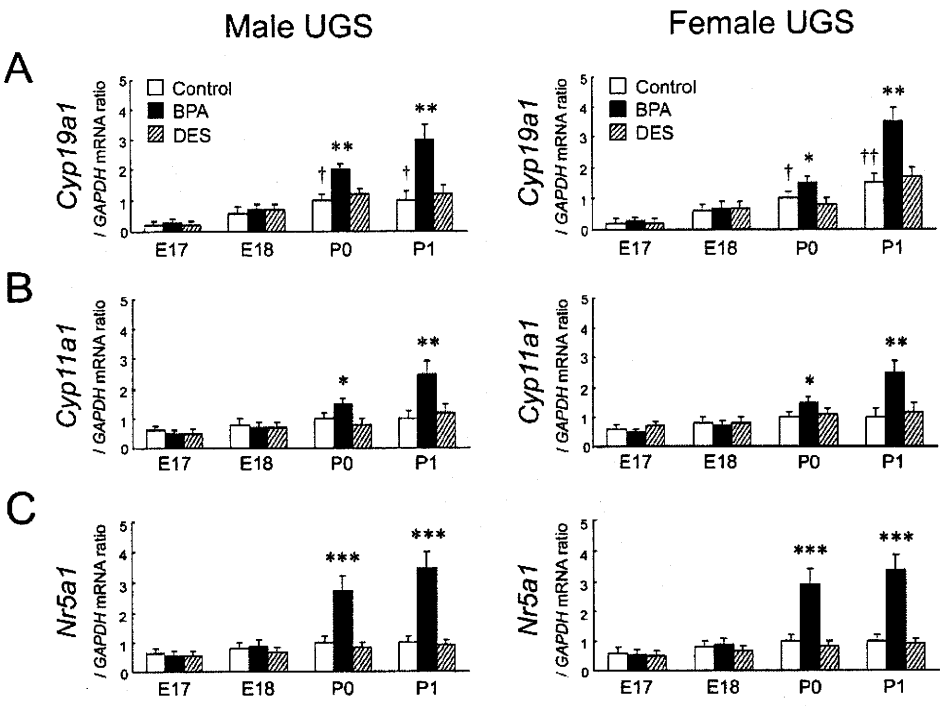

FIG. 2. BPA-specific up-regulation of steroidogenic enzyme and sex-determining gene mRNA in mouse UGS. The relative mRNA expressions of *Cyp19a1* (**A**), *Cyp11a1* (**B**), and *Nr5a1* (**C**) were determined in the untreated control (open bar), BPA-treated UGA (closed bar), and DES-treated UGS (slashed bar) between E17 and P1. $^{*}P < 0.05$, $^{**}P < 0.01$, $^{***}P < 0.001$ vs. control at each time point; $^{\dagger}P < 0.01$, $^{\dagger\dagger}P < 0.001$ vs. control at E17.

untreated male and female UGS, the mRNA of *Cyp19a1* was gradually increased between E17 and P1.

Restricted BPA-Specific Up-Regulation of Steroidogenic Enzyme and Sex-Determining Gene mRNA in UGE and UGM

In male fetuses at P1, it was not feasible to separate UGE and UGM components within the male UGS because of the formation of prostatic buds. In the female at P1, the up-regulation of *Cyp19a1*, *Cyp11a1*, and *Nr5a1* mRNA was observed only in UGM, not in UGE, of the BPA-treated group (Fig. 3). In both male and female UGE, expressions of such mRNAs were quite low and not up-regulated, even in the BPA-treated group. At E17, no difference in mRNA expression levels was found when comparing the untreated male UGM with that of the female.

BPA-Specific Increases of Aromatase-Expressing Cells in Primary Cultured UGM

In both the male and female, P1 UGM was primary cultured in vitro. Representative pictures of aromatase-positive cells are shown in Figure 4, A–C. The aromatase-positive staining was

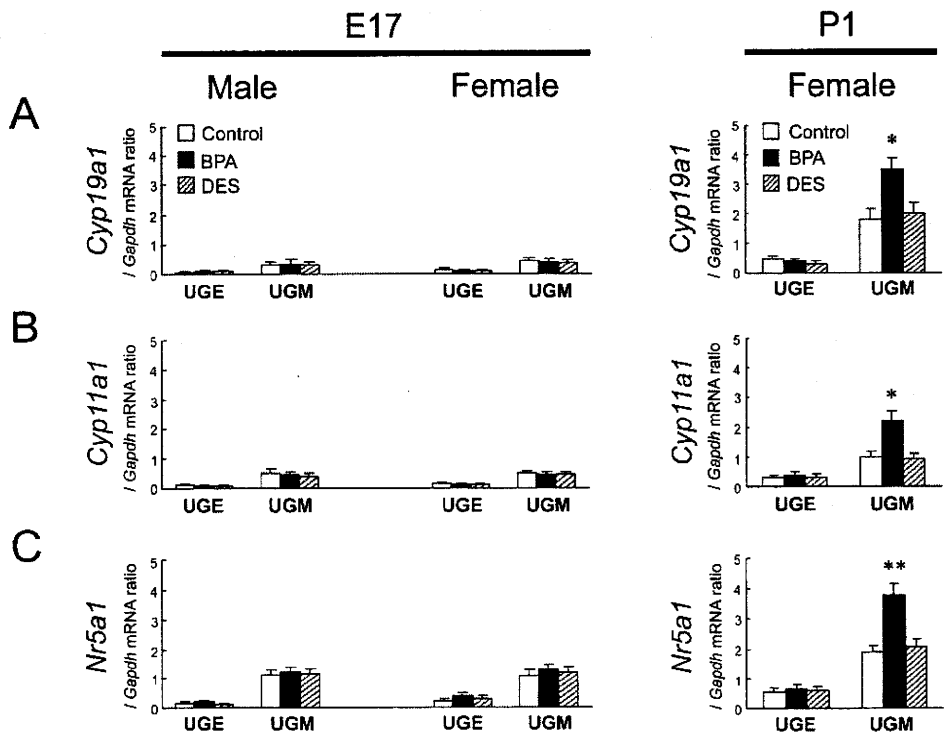

FIG. 3. Restricted BPA-specific up-regulation of steroidogenic enzyme and sex-determining gene mRNA in UGE and UGM. The relative mRNA expressions of *Cyp19a1* (**A**), *Cyp11a1* (**B**), and *Nr5a1* (**C**) were determined for UGE and UGM of the untreated control (open bar), BPA-treated UGS (closed bar), and DES-treated UGS (slashed bar) at E17 and P1. $^{*}P < 0.01$, $^{**}P < 0.001$ vs. control.

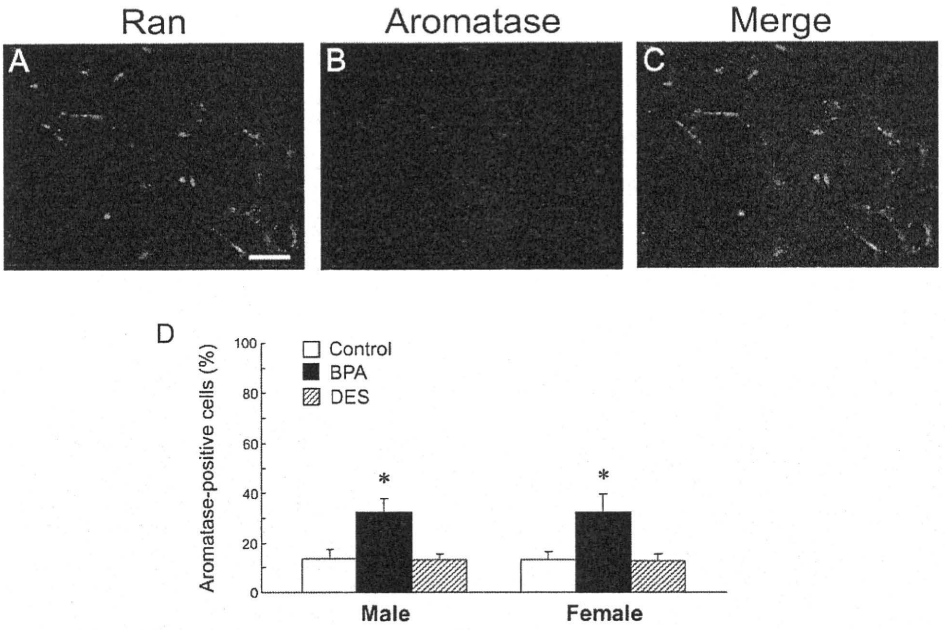

FIG. 4. BPA-specific increases of aromatase-expressing cells in primary cultured UGM. **A–C**) Fluorescence signals were detected for the CYP19A1 (aromatase) protein in primary cultured UGM. The nuclei were identified by Ran staining. Bar = 100 μm, magnification ×400. **D**) The number of aromatase-positive cells was counted in primary cultured UGM of the untreated control open bar), BPA-treated UGS (closed bar), and DES-treated UGS (slashed bar), and the percentage of aromatase-positive cells was calculated from at least 10 areas. $*P < 0.01$ vs. control.

observed in the cytoplasm of cultured UGM. The rate of positivity (i.e., the percentage of cells that expressed CYP19A1 [aromatase] protein), was approximately 10% in the untreated and the DES-treated groups, whereas it was as high as approximately 30% in the BPA-treated group (Fig. 4D). No difference in the rate of positivity of CYP19A1 (aromatase) was found when comparing the untreated male UGM to that of the female.

Restricted BPA-Specific Up-Regulation of Esrrg *mRNA in UGE and UGM*

In E17 female UGM, the mRNA expression of *Esr1* was up-regulated by both BPA and DES treatment (Fig. 5A). At E17, however, the mRNA expression of *Ar* was up-regulated by both BPA and DES treatment in the male UGS (Fig. 5B). At P1, mRNA expression of *Ar* was up-regulated by both BPA and DES treatment in the female UGS (Fig. 5B). In both the male and female, the up-regulation of *Esrrg* mRNA was observed at E17 and restricted in UGM, but not in UGE, of the BPA-treated group (Fig. 5C). In both the male and female UGE, the expression of *Esrrg* mRNA was quite low and not up-regulated, even in the BPA-treated group. At E17, no difference in mRNA expression levels was found when comparing the untreated male UGS with that of the female.

BPA-Specific Increases of ESRRG-Expressing Cells in Primary Cultured UGM

In both the male and female, E17 UGM was primary cultured in vitro. Representative pictures of ESRRG-positive

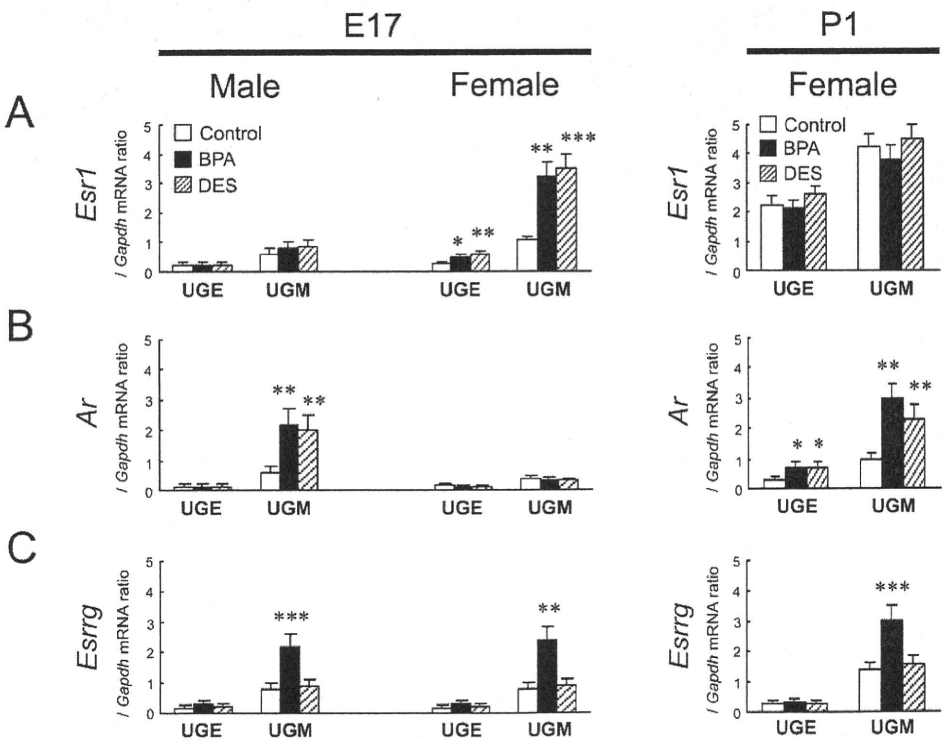

FIG. 5. Restricted BPA-specific up-regulation of *Esrrg* mRNA in UGE and UGM. The relative mRNA expressions of *Esr1* (**A**), *Ar* (**B**), and *Esrrg* (**C**) were determined in UGE and UGM of the untreated control (open bar), BPA-treated UGS (closed bar), and DES-treated UGS (slashed bar) at E17 and P1. $*P < 0.05$, $**P < 0.01$, $***P < 0.001$ vs. control.

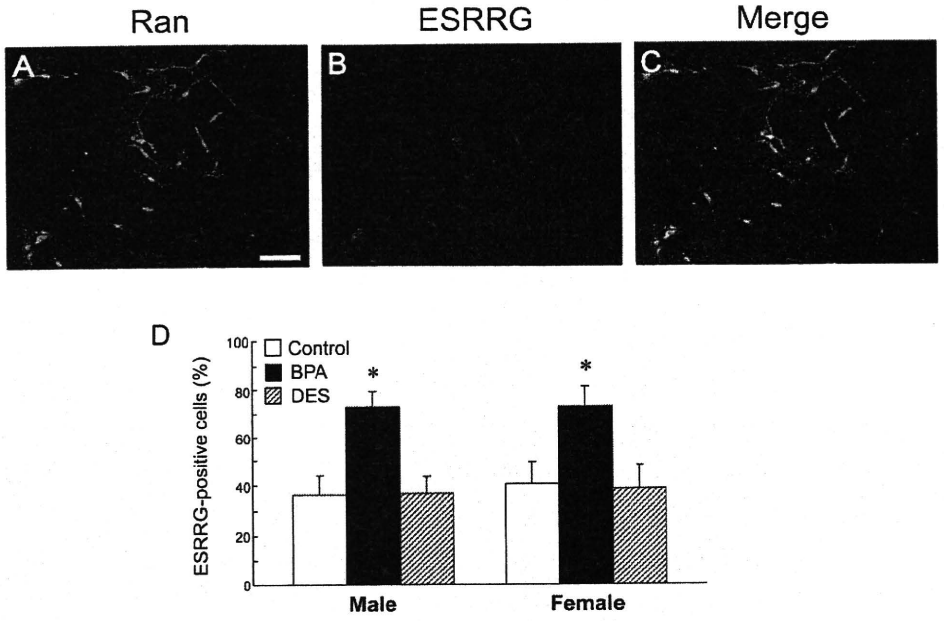

FIG. 6. BPA-specific increases of ESRRG-expressing cells in primary cultured UGM. **A–C**) Fluorescence signals were detected for the ESRRG protein in primary cultured UGM. The nuclei were identified by Ran staining. Bar = 100 μm, magnification ×400. **D**) The number of ESRRG-positive cells was counted in primary cultured UGM of the untreated control (open bar), BPA-treated UGS (closed bar), and DES-treated UGS (slashed bar), and the percentage of ESRRG-positive cells was calculated from at least 10 areas. $*P < 0.01$ vs. control.

cells are shown in Figure 6, A–C. The ESRRG-positive staining was observed in both the nucleus and the cytoplasm of cultured UGM. The number of ESRRG-positive UGM was significantly increased only in the BPA-treated group and showed a 2.2-fold increase in males and a 1.6-fold increase in females (Fig. 6D). No difference was found in the rate of positivity of ESRRG when comparing the untreated male UGM with that of the female.

BPA-Specific Up-Regulation of Esrrg *and Steroidogenic Enzyme mRNA in Sex Hormone-Related Organs*

To investigate the BPA-specific up-regulation of in situ steroidogenesis in other organs, we first examined the changes in *Esrrg* mRNA expression in sex hormone-related organs, such as the cerebellum, heart, kidney, ovary, and testis. At P1, the mRNA expression of *Esr1* in the cerebellum, heart, kidney, and ovary, but not in the testis, was up-regulated by both BPA and DES treatment (Fig. 7A). However, no significant difference in *Ar* mRNA expression was observed in all organs examined (Fig. 7B). In the untreated group, the mRNA expression of *Esrrg* was not detected in the testis at E17 and P1 (Fig. 7C). The up-regulation of *Esrrg* mRNA was observed at E17 and restricted to the cerebellum, heart, kidney, and ovary (Fig. 7C). The BPA-specific up-regulation of *Cyp19a1*, *Cyp11a1*, and *Nr5a1* mRNA was observed only at P1 in the cerebellum, heart, kidney, and ovary, but not in the testis (Fig. 8).

DISCUSSION

Concern about the effects of EDCs such as BPA on human health has been increasing [24]. Although the majority of EDCs have the potential to alter functioning of the reproductive and endocrine system, the actual mechanism responsible for such alterations has not been identified thoroughly. BPA is of concern because its chemical structure resembles that of DES. Several studies have reported that BPA can mimic estrogen action, such as induction of vaginal cornification, uterine vascular permeability, growth and differentiation of the mammary gland, and synaptic plasticity in the hippocampus [25–28]. In the prostate, alterations in normal development can produce permanent changes that persist throughout adulthood and may increase the risk of disease in later life [9]. Thus, our objective was to investigate the biological effects of low-dose BPA on the initial development of primary ducts in the fetal prostate.

During prostatic development, alteration of sex steroid hormone synthesis may be responsible for prostatic anomalies associated with fetal exposure to EDCs. In the present study, fetal exposure to low-dose BPA increased E_2 levels in P1 UGS of both the male and female, whereas DES-induced changes were not detected. This alteration was also correlated with increased activity of CYP19A1 (aromatase) in UGS at P1, suggesting the unique action of BPA for in situ steroidogenesis in UGS. The BPA-specific increase of E_2 levels in UGS at P1 was correlated with the following: mRNA up-regulation of steroidogenic enzymes, such as *Cyp19a1* and *Cyp11a1*, and an increased number of aromatase-expressing UGM. The enzyme CYP19A1 (aromatase) is responsible for in situ E_2 production and the crucial testosterone/E_2 balance necessary for normal embryonic and fetal development, even in males. The data presented here shows that the up-regulation of *Cyp19a1* mRNA in BPA-treated UGM was comparable to changes in both in situ E_2 production and CYP19A1 (aromatase) activity.

In the present study, we demonstrated that the BPA-specific increase in steroidogenic enzyme mRNA and aromatase-expressing cell number were observed in both the male and female UGM. During embryonic development, the mesenchymal component is involved in the induction and organogenesis of various organs, including the prostate, mammary gland, lung, kidney, and pancreas. It has been well established that subpopulations of the mesenchymal component are a source of potent molecules that regulate epithelial growth and differentiation [29]. In the prostate, androgen-responsive signals derived from UGM permissively and instructively induce UGE to form primary ducts of the prostate [30].

Comparison between the neonatal male and female UGS shows a similarity in the condensed mesenchyme of the ventral areas—that is, the ventral prostate mesenchyme (VPM) in the male and the ventral mesenchymal pad (VMP) in the female [31]. In the male, a defined VPM is specifically associated with ductal branching morphogenesis and cytodifferentiation of the ventral prostate. Females do not usually form a prostate. In a

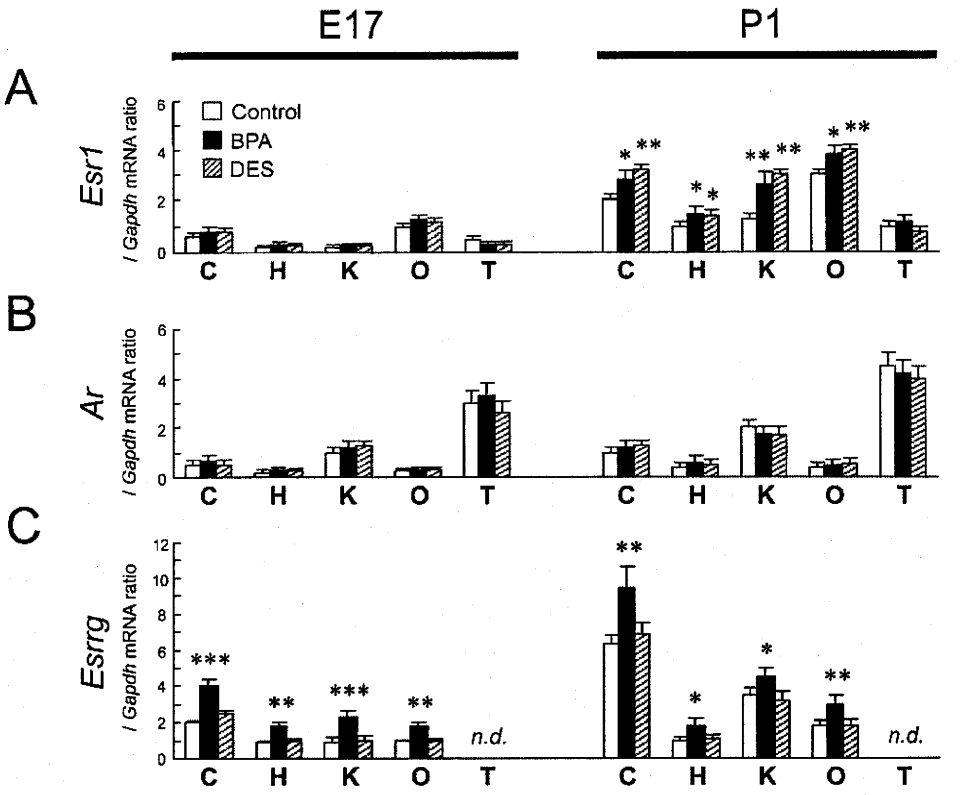

FIG. 7. BPA-specific up-regulation of *Esrrg* mRNA in sex steroid hormone-related organs. The relative mRNA expressions of *Esr1* (**A**), *Ar* (**B**), and *Esrrg* (**C**) were determined in sex steroid hormone-related organs of the untreated control (open bar), BPA-treated UGS (closed bar), and DES-treated UGS (slashed bar) at E17 and P1. C, cerebellum; H, heart; K, kidney; O, ovary; T, testis; *n.d.*, not detected. $^{*}P < 0.05$, $^{**}P < 0.01$, $^{***}P < 0.001$ vs. control.

tissue recombination model, the female VMP induces prostate development in response to androgens [32], suggesting that cells within the female VMP have prostatic-inductive activity. Moreover, an earlier tissue recombination study showed that the ability of the female UGS to respond to androgens in forming prostate was gradually lost between P1 and P5 [33]. These results suggest strongly that androgen-responsive regulatory molecules are expressed constitutively even in the female VMP. Although the female VMP forms in the absence of androgens, androgen receptor (AR) expression was observed in the neonatal female VMP in a pattern similar to that observed in the male VPM [34]. Therefore, the BPA-specific increase in E_2 levels might interact with the intracellular AR signaling in both the male VPM and the female VMP. However, to our knowledge,

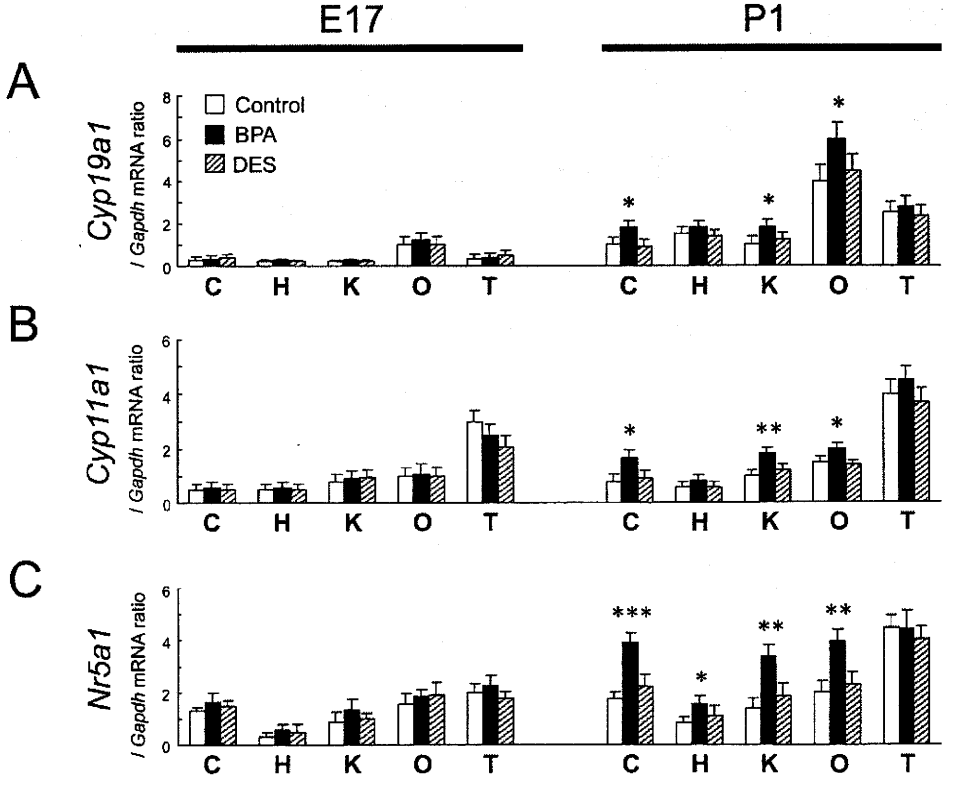

FIG. 8. BPA-specific up-regulation of steroidogenic enzyme and sex-determining gene mRNA in sex steroid hormone-related organs. The relative mRNA expressions of *Cyp19a1* (**A**), *Cyp11a1* (**B**), and *Nr5a1* (**C**) were determined in sex steroid hormone-related organs of the untreated control (open bar), BPA-treated UGS (closed bar), and DES-treated UGS (slashed bar) at E17 and P1. C, cerebellum; H, heart; K, kidney; O, ovary; T, testis. $^{*}P < 0.05$, $^{**}P < 0.01$, $^{***}P < 0.001$ vs. control.

the morphological changes in neonatal female UGS have not yet been investigated.

Our results suggest that BPA has a stimulatory effect on in situ steroidogenesis in P1 UGS of both the male and female at low-dose exposure levels. Recently, ESRRG has been reported to bind strongly with BPA [35]. Susens et al. [36] have reported that expression of ESRRG in the mouse is organ-specific: ESRRG is expressed in the brain, heart, kidney, and skeletal muscle but not in the lung, spleen, and testis. In the present study, the up-regulation of *Cyp19a1* and *Cyp11a1* mRNA by BPA treatment was detected only in organs expressing *Esrrg* mRNA. These data suggest that the possibility of a stimulatory effect on in situ steroidogenesis by fetal exposure to low-dose BPA may be a concern not only in UGS but also in organs expressing ESRRG, such as the brain, heart, kidney, and ovary. It is important to note that Takeda et al. [23] have recently reported that ESRRG was detected in the human testis, suggesting that the distribution of ESRRG differs slightly between mice and humans.

In the present study, the BPA-specific up-regulation of steroidogenic enzyme mRNA in UGS, cerebellum, heart, kidney, and ovary was observed only during the neonatal period (i.e., P0 and P1) and not during the prenatal period (i.e., E17 and E18). During pregnancy in rodents, large amounts of estrogens produced in the maternal ovaries are continuously delivered to the fetus through the placenta. After birth, however, the fetus may be released from the maternal, high-estrogen environment. Thus, one possibility is that the maternal, high-estrogen environment in pregnancy may protect the fetus from the effect of BPA on in situ steroidogenesis during the prenatal period. However, we did not investigate the effects of neonatal BPA treatment on in situ steroidogenesis.

The EDC-induced alterations of the in situ estrogen environment depend on each compound. In addition to atrazine and dioxin, the organotin compound tributyltin also increases E_2 production in human placental choriocarcinoma cells [37]. Tributyltin has been demonstrated to induce the superimposition of male sex organs, such as a penis and/or a vas deferens, over female sex organs, which is a phenomenon known as imposex [38]. These studies suggest strongly that EDCs might affect fetal development not only by mimicking the actions of sex steroid hormones but also by alteration of in situ steroidogenesis.

In the prostate, AR expressed in mesenchyme is required for directing growth and branching morphogenesis of epithelia, presumably by induction of growth factors [39]. In the present study, fetal exposure to BPA or DES increased *Ar* mRNA expression in E17 UGM of the male, whereas *Esr1* mRNA expression was up-regulated in E17 UGM of the female. Recently, Richter et al. [40] have reported that in vitro BPA treatment stimulates *Ar* and *Esr1* mRNA expression in mesenchymal cells isolated from fetal mouse prostate. Thus, our results support the idea that BPA-induced cell proliferation of the primary prostatic ducts may be caused by inducing *Ar* mRNA expression in the male UGM. In contrast, the induction of *Esr1* mRNA expression by BPA or DES may create a positive-feedback loop in the female UGM. Further investigation and morphological analysis will be necessary to confirm the effects of up-regulated ESR1 in the female UGS.

In conclusion, we have shown the unique action of BPA in the mouse UGS. Specifically, we have demonstrated that the increases in E_2 levels and CYP19A1 (aromatase) activity were observed in the BPA-treated UGS but not in the DES-treated UGS. Ricke et al. [41] have recently reported that stromal hormone imbalance, a potential source of local E_2 production, may be responsible for prostatic disease, such as benign prostatic hyperplasia and prostate cancer. The data in the present study give rise to the concept that the development and differentiation of UGS in mouse fetuses is very sensitive to fetal exposure to low-dose BPA via the mother. Further investigation of various aspects of BPA-specific action is necessary to fully understand the role of BPA as an EDC.

ACKNOWLEDGMENTS

We thank Prof. Nobuhiro Harada at Department of Biochemistry, Fujita Health University School of Medicine, Aichi, Japan, for kindly providing rabbit polyclonal antiaromatase antibody. We also thank Mrs. Hiroko Nishii for technical support.

REFERENCES

1. Sekizawa J. Low-dose effects of bisphenol A: a serious threat to human health? J Toxicol Sci 2008; 33:389–403.
2. Newbold RR, Jefferson WN, Padilla-Banks E. Prenatal exposure to bisphenol A at environmentally relevant doses adversely affects the murine female reproductive tract later in life. Environ Health Perspect 2009; 117:879–885.
3. McPherson SJ, Ellem SJ, Risbridger GP. Estrogen-regulated development and differentiation of the prostate. Differentiation 2008; 76:660–670.
4. Welshons WV, Nagel SC, vom Saal FS. Large effects from small exposures. III. Endocrine mechanisms mediating effects of bisphenol A at levels of human exposure. Endocrinology 2006; 147:S56–S69.
5. Schonfelder G, Wittfoht W, Hopp H, Talsness CE, Paul M, Chahoud I. Parent bisphenol A accumulation in the human maternal-fetal-placental unit. Environ Health Perspect 2002; 110:A703–A707.
6. Tsutsumi O. Assessment of human contamination of estrogenic endocrine-disrupting chemicals and their risk for human reproduction. J Steroid Biochem Mol Biol 2005; 93:325–330.
7. Timms BG, Howdeshell KL, Barton L, Bradley S, Richter CA, vom Saal FS. Estrogenic chemicals in plastic and oral contraceptives disrupt development of the fetal mouse prostate and urethra. Proc Natl Acad Sci U S A 2005; 102:7014–7019.
8. Ogura Y, Ishii K, Kanda H, Kanai M, Arima K, Wang Y, Sugimura Y. Bisphenol A induces permanent squamous change in mouse prostatic epithelium. Differentiation 2007; 75:745–756.
9. Ho SM, Tang WY, Belmonte de Frausto J, Prins GS. Developmental exposure to estradiol and bisphenol A increases susceptibility to prostate carcinogenesis and epigenetically regulates phosphodiesterase type 4 variant 4. Cancer Res 2006; 66:5624–5632.
10. Markey CM, Luque EH, Munoz de Toro M, Sonnenschein C, Soto AM. In utero exposure to bisphenol A alters the development and tissue organization of the mouse mammary gland. Biol Reprod 2001; 65: 1215–1223.
11. Honma S, Suzuki A, Buchanan DL, Katsu Y, Watanabe H, Iguchi T. Low-dose effect of in utero exposure to bisphenol A and diethylstilbestrol on female mouse reproduction. Reprod Toxicol 2002; 16:117–122.
12. Kubo K, Arai O, Omura M, Watanabe R, Ogata R, Aou S. Low-dose effects of bisphenol A on sexual differentiation of the brain and behavior in rats. Neurosci Res 2003; 45:345–356.
13. Fan W, Yanase T, Morinaga H, Gondo S, Okabe T, Nomura M, Komatsu T, Morohashi K, Hayes TB, Takayanagi R, Nawata H. Atrazine-induced aromatase expression is SF-1 dependent: implications for endocrine disruption in wildlife and reproductive cancers in humans. Environ Health Perspect 2007; 115:720–727.
14. Baba T, Mimura J, Nakamura N, Harada N, Yamamoto M, Morohashi K, Fujii-Kuriyama Y. Intrinsic function of the aryl hydrocarbon (dioxin) receptor as a key factor in female reproduction. Mol Cell Biol 2005; 25: 10040–10051.
15. Moustafa GG, Ibrahim ZS, Hashimoto Y, Alkelch AM, Sakamoto KQ, Ishizuka M, Fujita S. Testicular toxicity of profenofos in matured male rats. Arch Toxicol 2007; 81:875–881.
16. Song KH, Lee K, Choi HS. Endocrine disrupter bisphenol A induces orphan nuclear receptor Nur77 gene expression and steroidogenesis in mouse testicular Leydig cells. Endocrinology 2002; 143:2208–2215.
17. Mlynarcikova A, Kolena J, Fickova M, Scsukova S. Alterations in steroid hormone production by porcine ovarian granulosa cells caused by bisphenol A and bisphenol A dimethacrylate. Mol Cell Endocrinol 2005; 244:57–62.
18. Hojo Y, Higo S, Ishii H, Ooishi Y, Mukai H, Murakami G, Kominami T, Kimoto T, Honma S, Poirier D, Kawato S. Comparison between

hippocampus-synthesized and circulation-derived sex steroids in the hippocampus. Endocrinology 2009; 150:5106–5112.
19. Nakanishi T, Nishikawa J, Hiromori Y, Yokoyama H, Koyanagi M, Takasuga S, Ishizaki J, Watanabe M, Isa S, Utoguchi N, Itoh N, Kohno Y, et al. Trialkyltin compounds bind retinoid X receptor to alter human placental endocrine functions. Mol Endocrinol 2005; 19:2502–2516.
20. Kanno J, Aisaki K, Igarashi K, Nakatsu N, Ono A, Kodama Y, Nagao T. "Per cell" normalization method for mRNA measurement by quantitative PCR and microarrays. BMC Genomics 2006; 7:64–77.
21. Ishii K, Imanaka-Yoshida K, Yoshida T, Sugimura Y. Role of stromal tenascin-C in mouse prostatic development and epithelial cell differentiation. Dev Biol 2008; 324:310–319.
22. Jakab RL, Horvath TL, Leranth C, Harada N, Naftolin F. Aromatase immunoreactivity in the rat brain: gonadectomy-sensitive hypothalamic neurons and an unresponsive "limbic ring" of the lateral septum-bed nucleus-amygdala complex. J Steroid Biochem Mol Biol 1993; 44:481–498.
23. Takeda Y, Liu X, Sumiyoshi M, Matsushima A, Shimohigashi M, Shimohigashi Y. Placenta expressing the greatest quantity of bisphenol A receptor ERRgamma among the human reproductive tissues: predominant expression of type-1 ERRgamma isoform. J Biochem 2009; 146:113–122.
24. vom Saal FS, Akingbemi BT, Belcher SM, Birnbaum LS, Crain DA, Eriksen M, Farabollini F, Guillette LJ Jr, Hauser R, Heindel JJ, Ho SM, Hunt PA, et al. Chapel Hill Bisphenol A Expert Panel Consensus Statement: integration of mechanisms, effects in animals and potential to impact human health at current levels of exposure. Reprod Toxicol 2007; 24:131–138.
25. Steinmetz R, Mitchner NA, Grant A, Allen DL, Bigsby RM, Ben-Jonathan N. The xenoestrogen bisphenol A induces growth, differentiation, and c-fos gene expression in the female reproductive tract. Endocrinology 1998; 139:2741–2747.
26. Milligan SR, Balasubramanian AV, Kalita JC. Relative potency of xenobiotic estrogens in an acute in vivo mammalian assay. Environ Health Perspect 1998; 106:23–26.
27. Colerangle JB, Roy D. Profound effects of the weak environmental estrogen-like chemical bisphenol A on the growth of the mammary gland of Noble rats. J Steroid Biochem Mol Biol 1997; 60:153–160.
28. Kawato S. Endocrine disrupters as disrupters of brain function: a neurosteroid viewpoint. Environ Sci 2004; 11:1–14.
29. Donjacour AA, Cunha GR. Stromal regulation of epithelial function. Cancer Treat Res 1991; 53:335–364.
30. Hayashi N, Cunha GR, Parker M. Permissive and instructive induction of adult rodent prostatic epithelium by heterotypic urogenital sinus mesenchyme. Epithelial Cell Biol 1993; 2:66–78.
31. Thomson AA. Role of androgens and fibroblast growth factors in prostatic development. Reproduction 2001; 121:187–195.
32. Timms BG, Lee CW, Aumuller G, Seitz J. Instructive induction of prostate growth and differentiation by a defined urogenital sinus mesenchyme. Microsc Res Tech 1995; 30:319–332.
33. Cunha GR. Age-dependent loss of sensitivity of female urogenital sinus to androgenic conditions as a function of the epithelia-stromal interaction in mice. Endocrinology 1975; 97:665–673.
34. Thomson AA, Timms BG, Barton L, Cunha GR, Grace OC. The role of smooth muscle in regulating prostatic induction. Development 2002; 129: 1905–1912.
35. Takayanagi S, Tokunaga T, Liu X, Okada H, Matsushima A, Shimohigashi Y. Endocrine disruptor bisphenol A strongly binds to human estrogen-related receptor gamma (ERRgamma) with high constitutive activity. Toxicol Lett 2006; 167:95–105.
36. Susens U, Hermans-Borgmeyer I, Borgmeyer U. Alternative splicing and expression of the mouse estrogen receptor-related receptor gamma. Biochem Biophys Res Commun 2000; 267:532–535.
37. Nakanishi T, Kohroki J, Suzuki S, Ishizaki J, Hiromori Y, Takasuga S, Itoh N, Watanabe Y, Utoguchi N, Tanaka K. Trialkyltin compounds enhance human CG secretion and aromatase activity in human placental choriocarcinoma cells. J Clin Endocrinol Metab 2002; 87:2830–2837.
38. Horiguchi T. Masculinization of female gastropod mollusks induced by organotin compounds, focusing on mechanism of actions of tributyltin and triphenyltin for development of imposex. Environ Sci 2006; 13:77–87.
39. Cunha GR, Donjacour A. Stromal-epithelial interactions in normal and abnormal prostatic development. Prog Clin Biol Res 1987; 239:251–272.
40. Richter CA, Taylor JA, Ruhlen RL, Welshons WV, Vom Saal FS. Estradiol and bisphenol A stimulate androgen receptor and estrogen receptor gene expression in fetal mouse prostate mesenchyme cells. Environ Health Perspect 2007; 115:902–908.
41. Ricke WA, McPherson SJ, Bianco JJ, Cunha GR, Wang Y, Risbridger GP. Prostatic hormonal carcinogenesis is mediated by in situ estrogen production and estrogen receptor alpha signaling. FASEB J 2008; 22: 1512–1520.

Pigment-Dispersing Factor Affects Nocturnal Activity Rhythms, Photic Entrainment, and the Free-Running Period of the Circadian Clock in the Cricket *Gryllus bimaculatus*

Ehab Hassaneen,[*,†] Alaa El-Din Sallam,[†] Ahmad Abo-Ghalia,[†]
Yoshiyuki Moriyama,[*] Svetlana G. Karpova,[*,1] Salah Abdelsalam,[*,2]
Ayami Matsushima,[‡] Yasuyuki Shimohigashi,[‡] and Kenji Tomioka[*,3]

[*]*Graduate School of Natural Science and Technology, Okayama University, Okayama, Japan,*
[†]*Zoology Department, Faculty of Science, Suez Canal University, Ismailia, Egypt, and*
[‡]*Graduate School of Sciences, Kyushu University, Fukuoka, Japan*

Abstract Pigment-dispersing factor (PDF) is a neuropeptide widely distributed in insect brains and plays important roles in the circadian system. In this study, we used RNA interference to study the role of the *pigment-dispersing factor* (*pdf*) gene in regulating circadian locomotor rhythms in the cricket, *Gryllus bimaculatus*. Injections of *pdf* double-stranded RNA (ds*pdf*) effectively knocked down the *pdf* mRNA and PDF peptide levels. The treated crickets maintained the rhythm both under light-dark cycles (LD) and constant darkness (DD). However, they showed rhythms with reduced nocturnal activity with prominent peaks at lights-on and lights-off. Entrainability of ds*pdf*-injected crickets was higher than control crickets as they required fewer cycles to resynchronize to the LD cycles shifted by 6 h. The free-running periods of the ds*pdf*-injected crickets were shorter than those of control crickets in DD. These results suggest that PDF is not essential for the rhythm generation but involved in control of the nocturnality, photic entrainment, and fine tuning of the free-running period of the circadian clock.

Key words circadian rhythm, entrainment, locomotor activity, nocturnality, pigment-dispersing factor, RNAi

Circadian rhythms are about 24-h periodicities widely observed in a variety of insect behaviors, such as locomotion (Abe et al., 1997; Tomioka et al., 1997), hatching (Tomioka et al., 1991; Sauman et al., 1996; Sakamoto and Tomioka, 2007), and eclosion (Chang, 2006). The neural mechanism controlling the overt rhythms still largely remains to be elucidated. The pigment-dispersing factor (PDF), an octadecaneuropeptide, has been reported as a key circadian neuromodulator/neurotransmitter functioning in the

1. Present address: Zoological Institute of Russian Academy of Sciences, St. Petersburg, Russia.
2. Present address: Zoology Department, Faculty of Science, Assuit University, Assuit, Egypt.
3. To whom all correspondence should be addressed: Kenji Tomioka, Graduate School of Natural Science and Technology, Okayama University, Okayama 700-853, Japan; e-mail: tomioka@cc.okayama-u.ac.jp.

JOURNAL OF BIOLOGICAL RHYTHMS, Vol. 26 No. 1, February 2011 3-13
DOI: 10.1177/0748730410388746

output pathway of the insect circadian networks regulating locomotor rhythms (Renn et al., 1999; Helfrich-Förster et al., 2000; Park et al., 2000; Isaac et al., 2007). In *Drosophila*, PDF is expressed in 16 cerebral clock neurons and required for normal circadian locomotor rhythms (Taghert et al., 2001; Taghert and Shafer, 2006). PDF is thus considered as the principal neurotransmitter of the clock neurons responsible for organizing daily locomotor rhythms. It is required to adjust cycling amplitude, period, and phase in a variety of clock neurons in the brain (Miyasako et al., 2007; Tomioka et al., 2008; Yoshii et al., 2009). The discovery of the PDF receptor gene (*pdfr*) and the behavioral analysis of *pdfr* mutants confirmed the critical role of PDF signaling in maintaining robust locomotor rhythms (Hyun et al., 2005; Lear et al., 2005; Mertens et al., 2005).

PDF plays important roles also in circadian rhythms of hemimetabolous insects. In cockroaches, it seems to be a primary neurotransmitter for regulation of the locomotor rhythm since transplantation of the accessory medulla including the PDF-immunoreactive neurons restores the locomotor rhythm in arrhythmic animals whose optic lobes had been removed (Reischig and Stengl, 2003). The importance of PDF is confirmed by the recent finding that *pdf* RNAi disrupted the circadian rhythmicity in German cockroaches (Lee et al., 2009). However, in the cricket, the regulatory role of PDF in overt locomotor rhythms remains to be examined since locomotor rhythm could be disrupted by removal of the outer half of the optic lobe without eliminating the PDF neurons in the proximal optic lobe (Okamoto et al., 2001).

Besides the regulatory role in locomotor activity, PDF regulates circadian responsiveness rhythms of the visual system. In the cricket, PDF levels undergo daily cycling in the optic lobe (Abdelsalam et al., 2008) and enhance the photoresponsiveness of the visually responding interneurons during night (Saifullah and Tomioka, 2003). Thus, PDF seems to be involved in fine tuning of behavioral rhythms under light-dark cycle as well as in photic entrainment. In fact, injection of PDF causes phase shifts of locomotor rhythms in a phase-dependent manner (Petri and Stengl, 1997; Singaravel et al., 2003). However, no detailed studies are available on the role of PDF in these light-associated behavioral regulations.

In this study, to elucidate the role of PDF in the cricket's circadian locomotor rhythm, we examined the profiles of circadian locomotor rhythms of *pdf* RNAi crickets, including the locomotor activity patterns in light-dark cycles and constant darkness, free-running period in constant darkness, and resynchronization to light-dark cycles shifted by 6 h. The results show that knocking down of the *pdf* mRNA and PDF peptide levels drastically reduced the nocturnal activity, accelerated resynchronization to shifted LDs, and shortened free-running periods in DD. Based on these results, we hypothesize the multiple roles of PDF in the cricket circadian system.

MATERIALS AND METHODS

Experimental Animals

Newly emerged adult male crickets, *Gryllus bimaculatus*, were used in all experiments. They were obtained from a laboratory colony maintained under standard environmental conditions: a lighting regimen of 12-h light and 12-h dark (LD12:12; light, 0600-1800 h; Japanese standard time) and a constant temperature of 25 °C. They were fed laboratory chow (CA-1, Nihon Clea, Tokyo, Japan) and water ad libitum.

RNA Interference

Double-stranded RNAs (dsRNA) for *Gryllus bimaculatus pdf (Gb'pdf)* and *DsRed2* were synthesized as previously described for the *Gb'per* gene using MEGAscript High Yield Transcription Kit (Ambion, Austin, TX) (Moriyama et al., 2008). A fragment (35-285 bp) of the *Gb'pdf* cDNA (GenBank accession no. AB047800), cloned into pBluescript II SK+ (Toyobo, Osaka, Japan), was amplified with M13 forward and reverse primers. *DsRed2* in pDsRed2-N1 (Clontech, Mountain View, CA), which is derived from a coral species (*Discosoma sp.*), was amplified with the forward and reverse primers containing T7 promoter. With these DNA fragments, RNAs were synthesized with T7 and T3 RNA polymerases. The same amounts of synthesized sense and antisense RNAs were mixed, denatured for 5 min at 98 °C, and annealed by a gradual cool down to room temperature. After ethanol precipitation, the obtained dsRNA was suspended in Ultra Pure Water (Invitrogen, Carlsbad, CA) at a concentration of 20 μM. The dsRNA solutions were stored at −80 °C until use. 759 nL of dsRNA solution was injected with a nanoliter injector (WPI, Sarasota, FL) into the thorax of newly emerged adult male crickets anesthetized with CO_2.

Quantification of mRNA Levels

Gb'pdf mRNA levels were measured using a quantitative real-time RT-PCR (qPCR). Total RNA was extracted from 20 adult male optic lobes with TRIzol Reagent (Invitrogen) and was treated with DNase I (Ambion) to remove contaminating genomic DNA. 450 ng of total RNA of each sample was reverse transcribed with random hexamers using PrimeScript RT reagent Kit (Perfect Real Time) (Takara Bio, Otsu, Japan). qPCR was performed with Mx3000P Real-Time PCR system (Stratagene, La Jolla, CA) using Fast Start Universal SYBR Green Master (ROX) (Roche, Basel, Switzerland) including SYBR Green with primers 5′-GCTGCTCGACAAGGAGGTAG-3′ and 5′-TTTCCGAGTTCCTTTTGTGG-3′. The *Gryllus bimaculatus ribosomal protein L18a* (*Gb'rpl18a*, GenBank accession no. DC448653) was used as an internal reference gene. The primers used for *Gb'rpl18a* were 5′-GCTCCGGATTACATCGTTGC-3′ and 5′-GCCAAATGCCGAAGTTCTTG-3′. The results were analyzed using the software associated with the instrument: quantification of mRNA levels was performed by the standard curve method (Rutledge and Cote, 2003). The values for *Gb'pdf* were normalized with the values for *Gb'rpl18a* at each time point. Results of 3 or 4 independent experiments were pooled to calculate the mean ± SEM.

Immunohistochemistry

For immunohistochemistry, dissected brains were fixed with 4% paraformaldehyde in 0.1 M phosphate buffer (pH 7.4) at 4 °C for about 12 h. After washing with phosphate-buffered saline (PBS), they were immersed overnight in a blocking buffer containing normal donkey serum. They were then incubated with rabbit polyclonal anti-*Gryllus* PDF (1/6000) for 72 h at 4 °C as previously described by Abdelsalam et al. (2008). Specimens were incubated in Cy3-conjugated goat anti-rabbit secondary antibodies (1/2000) (Jackson Immunoresearch, West Grove, PA). Preparations were washed with PBS containing 1% Triton X-100 between all steps. Brains were mounted in 50% glycerine (in PBS). Preparations were scanned and photographed with the Olympus Fluoview300 laser confocal imaging system (Tokyo, Japan). Photographs were taken at 2- and 4-μm intervals for the optic lobes and midbrain areas, respectively. PDF immunoreactivity in the cerebral lobes and optic lobes were calculated with ImageJ computer software

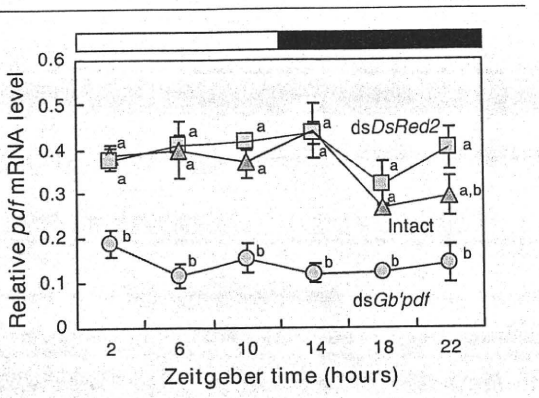

Figure 1. *Gb'pdf* **mRNA levels relative to** *Gb'rpl18a* **mRNA levels in the optic lobes of intact, ds*DsRed2*-injected control, and ds*Gb'pdf*-injected crickets under LD12:12 at 25 °C. Measurement was performed 5 days after the injection in case of injected crickets. mRNA levels were measured by quantitative real-time RT-PCR. The white and black bars indicate light and dark fractions of the LD cycle, respectively. Plotted are the mean ± SEM of 3 or 4 replicate samples; the mRNA in each sample was extracted from 20 optic lobes of 10 adult male crickets. Values with different letters significantly differ from each other ($p < 0.05$; ANOVA with Tukey test).**

(W. Rasband, National Institutes of Health, Bethesda, MD) by measuring the gray brightness value of the photographs. The background values were also measured and subtracted from the staining intensity. The values were obtained from 9 to 11 specimens for each time point and shown as mean ± SEM.

Behavioral Assay

Locomotor activity was monitored and recorded using a computerized system described previously (Moriyama et al., 2008). Newly emerged adults were individually housed in a transparent plastic box (18 × 9 × 4.5 cm) with a rocking substratum, of which movement caused by a moving cricket was detected by a magnetic reed switch placed on the bottom of the box. The number of rocking was recorded every 6 min by a computer. The actographs were placed in an incubator (MIR-153, Sanyo, Moriguchi, Japan), in which temperature was kept at 25 °C and lighting conditions were given by a cool white fluorescent lamp connected to an electric timer. The light intensity was 500 to 900 lux at the animal's level, varying with the proximity to the lamp. The raw data were displayed as conventional double-plotted actograms to evaluate activity patterns, and free-running periods were calculated by the χ^2 periodogram (Sokolove

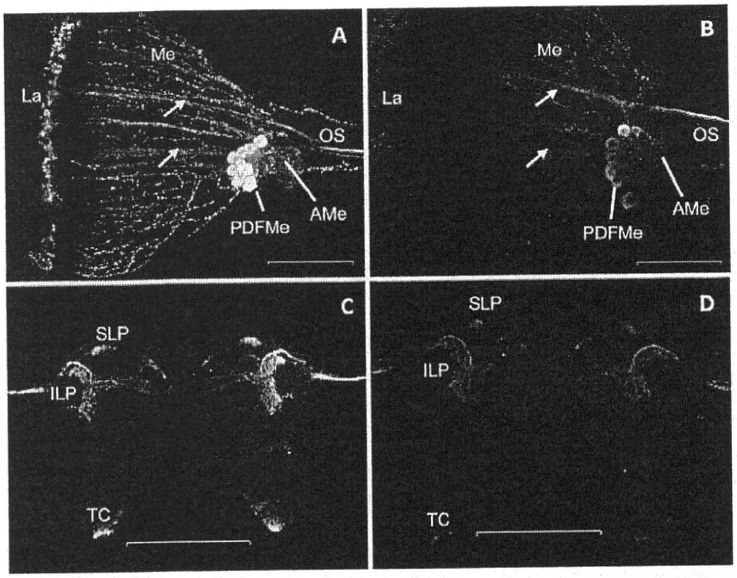

Figure 2. Confocal laser microscope images of the PDF-immunoreactive neurons in the optic lobes (A, B) and protocerebral lobe (C, D) of male crickets injected with ds*DsRed2* (A, C) or ds*Gb'pdf* (B, D). The neurons were labeled with anti-*Gryllus* PDF 10 days or 15 days after injection in optic and protocerebral lobes, respectively. Note the weaker immunoreactivity in ds*Gb'pdf*-treated specimens. Bars indicate 100 µm (A, B) and 500 µm (C, D). La = lamina; Me = medulla; OS = optic stalk; PDFMe = medulla PDF-immunoreactive cells; AMe = accessory medulla; SLP = superior lateral protocerebrum; ILP = inferior lateral protocerebrrm; TC = tritocerebrum. Arrows (A, B) point to axon bundles of PDFMe cells in the medulla.

and Bushell, 1978). In the periodograms, the peaks appearing above the 0.05 confidence level were designated as statistically significant.

The daytime and nighttime activities and the ratio of nighttime/daytime activity were calculated where necessary. In free-running conditions, the daily average activity profiles with 6-min resolution were first calculated with a free-running period. The onset of subjective night was determined when the activity exceeded the average activity level and the duration of the subjective night was set at 12 circadian hours. The subjective night/subjective day activity ratio was then calculated.

RESULTS

pdf RNAi Knocked Down *Gb'pdf* mRNA Levels in the Cricket's Optic Lobe

Levels of *Gb'pdf* mRNA transcripts were measured under LD12:12 in the optic lobes of intact, *DsRed2* dsRNA (ds*DsRed2*)–injected control and *Gb'pdf* dsRNA (ds*Gb'pdf*)–injected adult male crickets using qPCR (Fig. 1). In intact and ds*DsRed2*-injected crickets, *pdf* mRNA levels were rather stable except a decrease at ZT18; no significant changes were detected by ANOVA ($p > 0.05$). There was no significant difference between the intact and the ds*DsRed2*-injected crickets at all the examined zeitgeber times. For ds*Gb'pdf*-injected crickets, measurement was performed 5 days after injection. The results showed that the *Gb'pdf* mRNA levels were significantly suppressed to about 30% of the control crickets (ANOVA followed by Tukey test, $p < 0.05$), with an exception at ZT22, where the value was not significantly different from intact crickets; no daily changes were observed (ANOVA, $p > 0.05$).

pdf dsRNA Reduced PDF Immunoreactivity

Effects of ds*Gb'pdf* on PDF levels were examined by measuring intensity of PDF immunolabeling using anti-*Gryllus* PDF antibody. Levels of PDF immunoreactivity were measured, after 5, 10, 15, and 20 days of injection, at PDFMe cell bodies, accessory medulla, medulla, and lamina areas in the optic lobe and at superior lateral protocerebrum and inferior lateral protocerebrum in the protocerebral lobe with 7 to 10 samples. In *Gb'pdf* RNAi crickets, PDF levels were significantly reduced in both the optic lobe and the cerebral lobe (Figs. 2 and 3). In the optic lobe, a significant reduction was observed 5 days after injection in all measured areas, while in the protocerebral lobe, 10 days were required until a significant reduction was detected (Fig. 3). Further gradual reduction of immunoreactivity proceeded with days both in the optic lobe and protocerebral lobe. The same pattern of reduction was evident in the axonal bundles in the medulla area and the optic stalk and in the tritocerebrum area (data not shown). It is noteworthy that PDF immunoreactivity gradually decreased even in intact and ds*DsRed2*-injected crickets except cell bodies, where a high level of immunoreactivity was maintained throughout the examined period. The reduction probably related to aging. No significant differences were found in staining levels between intact and ds*DsRed2*-injected crickets in all examined tissues.

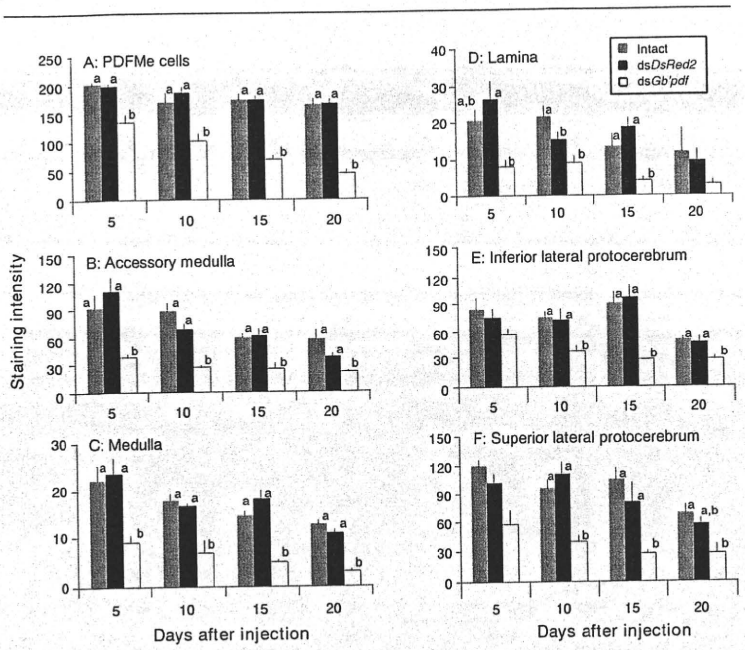

Figure 3. Effects of ds*Gb'pdf* on the PDF immunoreactivity in cell bodies of the PDFMe neurons (A), accessory medulla (B), medulla (C), lamina (D), inferior lateral protocerebrum (E), and superior lateral protocerebrum (F). Plotted are the mean ± SEM of 7 to 10 samples. Values with different letters significantly differ from each other ($p < 0.05$; ANOVA with Tukey test).

pdf RNAi Altered Circadian Locomotor Activity

To investigate the effects of *pdf* RNAi on the locomotor rhythm, we measured the locomotor activity in 76 male crickets injected with ds*Gb'pdf*. We also used 109 intact and 80 ds*DsRed2*-injected crickets as controls. The representative records of locomotor activity are shown in Figure 4. Analysis of activity levels for the first 13 days after imaginal molt revealed that *Gb'pdf* dsRNA significantly reduced activity during night time (Fig. 5). In intact and ds*DsRed2*-injected control crickets, average nighttime activity gradually increased from 20 to approximately 70 to 90 during the first 10 days (Fig. 5B). The daytime activity showed an increase from 40 to approximately 50 to 60 during the first 5 days, followed by a slight decrease (Fig. 5A). The night/day activity ratio increased rapidly between day 5 to day 10 to reach a peak level around 2.5 and then maintained the level thereafter (Fig. 5C). These changes are associated with a reversal from nymphal diurnality to adult nocturnality during the first several days after the imaginal molt (Tomioka and Chiba, 1982). The ds*Gb'pdf* RNAi crickets showed significantly less activity only for night time (Figs. 4, 5A and 5B). The night/day activity ratio only slightly increased and stayed at nearly 1 (Fig. 5C), being mostly significantly smaller than both ds*Gb'pdf* RNAi and intact crickets after 5 days of injection onwards (ANOVA followed by Tukey test, $p < 0.05$) (Fig. 5C).

pdf RNAi Resulted in a Faster Resynchronization to Shifted LD Cycles

Gb'pdf RNAi crickets showed shorter transient cycles required for resynchronization to LD cycles advanced or delayed by 6 h than intact and ds*DsRed2*-injected crickets (Figs. 4 and 6) (ANOVA followed by Tukey test, $p < 0.05$). *DsRed2* RNAi slightly increased the transient cycles only for delay shifts (Tukey test, $p < 0.05$). In intact and ds*DsRed2*-injected controls, a remarkable positive masking effect of light was observed at lights-on several days after phase advance of LD (Fig. 4A and 4C), while the positive masking associated with advance shifts was significantly reduced (79.0 ± 54.6 v. 137.5 ± 102.3 [*DsRed2* RNAi], *t* test, $p < 0.01$) and sometimes disappeared in the ds*Gb'pdf*-injected crickets (Fig. 4E). Weak masking effects of light were often observed even in these ds*Gb'pdf* RNAi crickets in steady-state entrainment (arrowheads in Fig. 4E and 4F).

pdf RNAi Shortened Free-Running Period in DD

To examine the effect of *Gb'pdf* RNAi on free-running rhythms under DD, we recorded the locomotor activity of 11 ds*Gb'pdf*-injected crickets under DD. The *Gb'pdf* RNAi crickets showed significantly shorter free-running periods than those of intact and ds*DsRed2*-injected crickets (ANOVA followed by Tukey test, $p < 0.05$) (Fig. 7). The ds*DsRed2*-injected crickets showed a slightly longer free-running period than intact crickets (Tukey test, $p < 0.05$). When activity was analyzed for free-running conditions, there were no significant differences in total daily activity and subjective night/subjective day activity ratio among the 3 groups of animals (ANOVA, $p > 0.05$) (Fig. 7E and 7F).

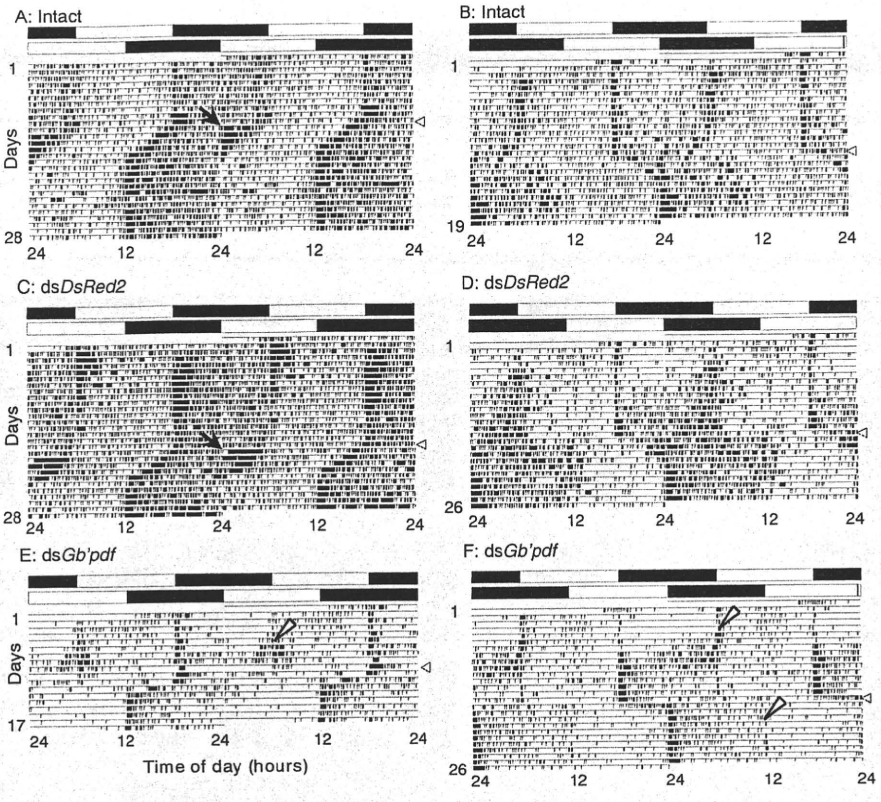

Figure 4. Double-plotted actograms of intact (A, B), ds*DsRed2*-injected (C, D), and ds*Gb'pdf*-injected crickets (E, F). Newly emerged intact or dsRNA-treated crickets were first kept in LD12:12 at 25 °C for about 10 days until full nocturnality is established, then subjected to either 6-h advance (A, C, E) or 6-h delay shifts (B, D, F) by shortening or lengthening the light phase, respectively. White and black bars indicate light and dark phases, respectively. Arrowheads indicate the day when LD was shifted. Arrows (A, C) indicate masking effect. White arrowheads indicate positive masking effects in ds*Gb'pdf*-injected crickets (E, F). Note the weak nocturnal activity levels and quicker resynchronization in *pdf* dsRNA-injected crickets.

DISCUSSION

Effectiveness of *pdf* RNAi

We showed here that a single injection of dsRNA of the *pdf* gene effectively knocked down its mRNA levels and subsequently its product PDF peptide levels, leading to altered circadian rhythms. The results of systemic *pdf* RNAi gene silencing are in accordance with a similar study on *pdf* in cockroaches (Lee et al., 2009) and on clock genes of crickets and other insects (Moriyama et al., 2008; Moriyama et al., 2009; Danbara et al., 2010; Kamae et al., 2010). Like clock genes *period* and *timeless* (Moriyama et al., 2008; Danbara et al., 2010), the effects of ds*Gb'pdf* continued for up to 4 weeks. The prolonged effect of *Gb'pdf* after a single injection might involve RNA-dependent RNA polymerase (RdRp) to convert the single-stranded target mRNA to dsRNA using the antisense strands of primary siRNAs as primers (Zamore et al., 2000; Lipardi et al., 2001; Sijen et al., 2001). This possibility is supported by a recent finding of RdRp in *Drosophila* (Lipardi and Paterson, 2009). The systemic RNAi thus provides an efficient way to unravel molecular machineries underlying various physiological functions by switching the genes "off" at the posttranscriptional level through a minimally invasive way. This is especially helpful for insects in which forward genetics is less practical comparable to *Drosophila*.

Injections of *pdf* dsRNA induced a gradual decrease of PDF immunoreactivity in both the optic lobe and protocerebrum (Figs. 2 and 3), indicating the reduction of PDF peptide levels. The gradual decrease is probably due to the lifetime of already present PDF because the mRNA level was strongly reduced on day 5 after the ds*pdf* injection (Fig. 1). Reduction of PDF in the neurons projecting into the protocerebrum seems important since these neurons are responsible for relaying the circadian output signal to the locomotor center located in the brain (Stengl and Homberg, 1994). Both daytime and nighttime activity reductions preceded the statistically significant reduction of PDF levels in the cerebral lobe (Figs. 3 and 5), suggesting that a slight decrease of PDF affects the locomotor activity. Thus, PDF seems to be an output neurotransmitter/neuromodulator for regulation of the locomotor activity as has been reported for *Drosophila* (Renn et al., 1999) and German cockroaches (Lee et al., 2009). In cockroaches, *pdf* RNAi effectively decreases PDF in the optic lobe and the brain below

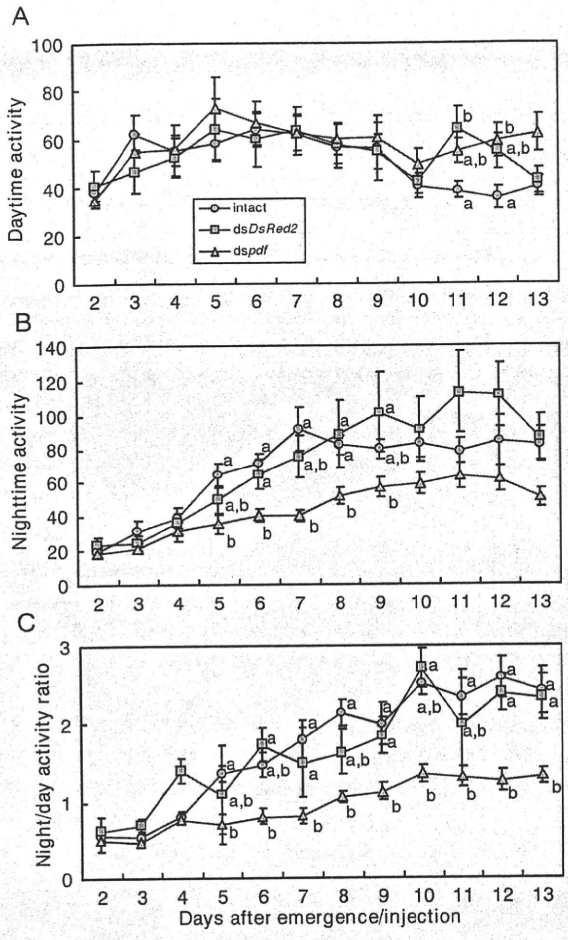

Figure 5. Effects of ds*Gb'pdf* RNAi on daily diurnal (A) and nocturnal activity (B) and night/day activity ratio (C) in the cricket *G. bimaculatus* in LD12:12. The abscissa represents days after injection of ds*Gb'pdf* or ds*DsRed2* or days after imaginal molt for intact crickets. Error bars indicate SEM. Values with different letters significantly differ from each other ($p < 0.05$; ANOVA with Tukey test).

the detectable level by immunohistochemistry within 10 days (Lee et al., 2009). However, in the present study, complete disappearance was never observed during 20 days after ds*pdf* injection. This might be attributable to species specificity in RNAi efficiency, the difference of expression levels of *pdf*, or the lifetime of PDF peptide. In the cricket, PDF peptide seems to have a very long lifetime because PDF immunoreactivity persisted in axons projecting to the optic stalk and protocerebral lobe for more than 30 days after the cell bodies were removed (Stengl, 1995; Okamoto et al., 2001).

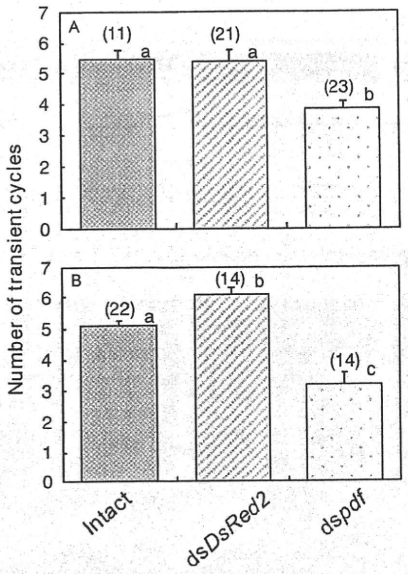

Figure 6. The average number of cycles required for resynchronization to LDs shifted by 6 h in the advance (A) or delay (B) direction in intact, ds*DsRed2*-injected, and ds*Gb'pdf*-injected crickets. Data are represented as mean ± SD. n = number of insects. Values with different letters significantly differ from each other ($p < 0.05$; ANOVA with Tukey test). Numbers in brackets indicate the number of animals used. Note that fewer numbers of cycles are required for resynchronization in ds*Gb'pdf*-injected crickets.

Possible Roles of PDF in the Cricket Circadian System

In contrast to the results in cockroaches where arrhythmicity was induced by *pdf* RNAi (Lee et al., 2009), the crickets treated with ds*pdf* maintained a clear locomotor rhythm in both LD and DD (Figs. 4 and 7). It is premature to exclude the possibility that PDF is indispensable for the circadian locomotor rhythm because our immunohistochemistry revealed that a still certain amount of PDF remains in both the optic lobes and protocerebrum (Figs. 2 and 3), whereas the PDF became below detectable level by immunohistochemistry within 10 days of ds*pdf* treatment in cockroaches (Lee et al., 2009). The preserved locomotor rhythm in the cricket might be attributable to the still remaining PDF. Several alterations of the locomotor rhythm were yet observed in *pdf* RNAi crickets. First, suppression of nocturnal activity was the most prominent feature of *pdf* RNAi crickets (Figs. 4 and 5). Second, *pdf* RNAi resulted in shortening of the free-running period under DD (Fig. 7). Third, the resynchronization to the LDs

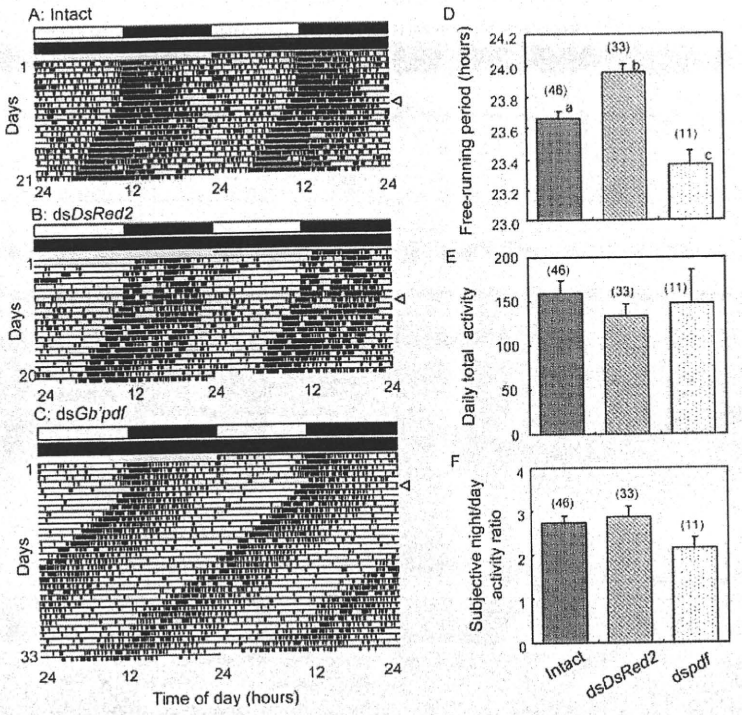

Figure 7. Representative free-running locomotor activity rhythms under DD in intact (A), ds*DsRed2*-injected (B), and ds*Gb'pdf*-injected crickets (C) and their average free-running periods (D), average daily total activity (E), and subjective night/subjective day activity ratio (F). White and black bars indicate light and dark phases of the LD cycle, respectively. Arrowheads indicated the day transferred to DD. *n* indicates the number of insects. Values with different letters significantly differ from each other ($p < 0.05$; ANOVA with Tukey test). Note the free-running period was significantly shorter in ds*Gb'pdf*-treated crickets.

shifted by 6 h occurs more quickly than control crickets (Fig. 4).

Gb'pdf RNAi suppressed nocturnal activity (Fig. 5), suggesting that PDF is released under the regulation of circadian clock as has been previously suggested (Saifullah and Tomioka, 2003; Abdelsalam et al., 2008). This fact is reminiscent of the finding that PDF regulates arousal in *Drosophila*: *pdf*^{01} flies have increased sleep (reduced locomotor activity) during the day (Parisky et al., 2008). The suppression of nocturnal activity in *pdf* RNAi crickets is consistent with what was observed in German cockroaches, where only nocturnal activity was reduced and eventually resulted in arrhythmicity (Lee et al., 2009). It could be thus hypothesized that PDF regulates the nocturnal activity in these nocturnal hemimetabolous insects. In *Drosophila pdf*^{01} mutant flies that genetically lack PDF, however, the evening peak is clearly maintained but with advanced phase, while the morning peak is generally absent (Renn et al., 1999; Blanchardon et al., 2001). Thus, the role of PDF in activity regulation seems different between diurnal and nocturnal insects. In this regard, the nymphal crickets *G. bimaculatus* seem a good subject to examine this hypothesis because they are diurnally active (Tomioka and Chiba, 1982).

The shortening of the free-running period under DD is consistent with the results in *pdf*^{01} *Drosophila* mutant flies, showing the free-running period much shorter than wild-type flies (Renn et al., 1999; Yoshii et al., 2009). PDF is hypothesized in *Drosophila* that it lengthens free-running periods and simultaneously couples the multiple clock neurons (Peng et al., 2003; Lin et al., 2004; Sheeba et al., 2008; Yoshii et al., 2009). A similar role of PDF is proposed in the cockroach (Schneider and Stengl, 2005). It seems likely that PDF lengthens the period of the molecular oscillation via the cAMP-dependent pathway (Shafer et al., 2008).

The quick resynchronization of *pdf* RNAi crickets to the shifted LDs suggests involvement of PDF in the photic entrainment pathway. It has been suggested that PDF regulates the circadian rhythm of the cricket's visual interneurons, which directly connect the bilateral medulla area of the optic lobe, increasing their photoresponsiveness during the night (Saifullah and Tomioka, 2003). This hypothesis is supported by the finding that *pdf* RNAi crickets showed reduced positive masking effect at lights-on during advance shifts after phase advance of LD by 6 h (Fig. 4) but seems to be inconsistent with the finding that reduction of PDF levels enhances the photic entrainability (Fig. 6). However, there are at least 2 possible explanations for the role of PDF in photic entrainment. First, the PDF enhances the photoresponsiveness of the visual interneurons, which may negatively act in the photic entrainment pathway. The second explanation is based on the *Drosophila* clock system including light-sensitive and relatively light-insensitive oscillators for the control of locomotor rhythm (Miyasako et al., 2007; Yoshii et al., 2009): a reduced level of PDF may weaken the PDF-dependent decelerating influence of light-insensitive oscillator on the light-sensitive oscillators, enabling the light-sensitive clock neurons to synchronize more

quickly. The other possibility is that extraretinal photoreception might be involved in the photic entrainment as has been suggested in the New Zealand weta and the band-legged crickets (Waddell et al., 1990; Shiga and Numata, 1997): reduced PDF levels may reduce the photic input through the visual system; then, input from the extraretinal entrainment pathway may become prominent. This might be plausible considering that *Drosophila* has multiple photoreceptive systems for photic entrainment including the compound eye, ocelli, H-B eyelet, and cryptochrome, an extraretinal photoreceptor (Rieger et al., 2003; Hanai and Ishida, 2009).

In addition to the entrainment pathway, PDF likely mediates direct effect of light. A startle response, or positive masking effect of light, occurring at lights-on after an advance shift of LD (Fig. 4A and 4C) was significantly reduced in *pdf* RNAi crickets (Fig. 4E). The startle response may be caused through the PDF pathway. The fact that no significant difference in activity levels was observed between *pdf* RNAi crickets and controls (Fig. 7) also suggests the PDF pathway regulates the activity in response to light. The PDF pathway probably plays a similar role in *Drosophila* because pdf^{01} mutant flies show only a weak morning peak (Yoshii et al., 2009) and the lLNvs that express PDF are responsible for the morning startle response (Sheeba et al., 2010). In summary, the PDF pathway plays multiple roles in the cricket circadian system, regulating the nocturnal rhythm, its photic entrainment, and the free-running period. With the aid of PDF, the cricket may maintain its robust nocturnal rhythm and adjust it to given LD cycles.

ACKNOWLEDGMENTS

This study was supported in part by grants to K.T. from the Japan Society for the Promotion of Science (JSPS). E.H. is supported by a grant from the Egyptian Ministry of Higher Education. Y.M. is a JSPS Research Fellow.

REFERENCES

Abdelsalam S, Uemura H, Umezaki Y, Saifullah ASM, Shimohigashi M, and Tomioka K (2008) Characterization of PDF-immunoreactive neurons in the optic lobe and cerebral lobe of the cricket, *Gryllus bimaculatus*. J Insect Physiol 54:1205-1212.

Abe Y, Ushirogawa H, and Tomioka K (1997) Circadian locomotor rhythms in the cricket, *Gryllodes sigillatus*. I: localization of the pacemaker and the photoreceptor. Zoolog Sci 14:719-727.

Blanchardon E, Grima B, Klarsfeld A, Chélot E, Hardin PE, Préat T, and Rouyer F (2001) Defining the role of *Drosophila* lateral neurons in the control of circadian activity and eclosion rhythms by targeted genetic ablation and PERIOD protein overexpression. Eur J Neurosci 13:871-888.

Chang DC (2006) Neural circuits underlying circadian behavior in *Drosophila melanogaster*. Behav Proc 71:211-225.

Danbara Y, Sakamoto T, Uryu O, and Tomioka K (2010) RNA interference of *timeless* gene does not disrupt circadian locomotor rhythms in the cricket *Gryllus bimaculatus*. J Insect Physiol 56:1738-1745.

Hanai S and Ishida N (2009) Entrainment of *Drosophila* circadian clock to green and yellow light by Rh1, Rh5, Rh6 and CRY. NeuroReport 20:755-758.

Helfrich-Förster C, Täuber M, Park JH, Mühling-Versen M, Schneuwly S, and Hofbauer A (2000) Ectopic expression of the neuropeptide pigment-dispersing factor alters behavioral rhythms in *Drosophila melanogaster*. J Neurosci 20:3339-3353.

Hyun S, Lee Y, Hong S-T, Bang S, Paik D, Kang J, Shin J, Lee J, Jeon K, Hwang S, et al. (2005) *Drosophila* GPCR Han is a receptor for the circadian clock neuropeptide PDF. Neuron 48:267-278.

Isaac RE, Johnson EC, Audsley N, and Shirras AD (2007) Metabolic inactivation of the circadian transmitter, pigment dispersing factor (PDF), by neprilysin-like peptidases in Drosophila. J Exp Biol 210:4465-4470.

Kamae Y, Tanaka F, and Tomioka K (2010) Molecular cloning and functional analysis of the clock genes, *Clock* and *cycle*, in the firebrat *Thermobia domestica*. J Insect Physiol 56:1291-1299.

Lear BC, Merrill CE, Lin J-M, Schroeder A, Zhang L, and Allada R (2005) A G protein-coupled receptor, groom-of-PDF, is required for PDF neuron action in circadian behavior. Neuron 48:221-227.

Lee C-M, Su M-T, and Lee H-J (2009) Pigment dispersing factor: an output regulator of the circadian clock in the german cockroach. J Biol Rhythms 24:35-43.

Lin Y, Stormo GD, and Taghert PH (2004) The neuropeptide pigment-dispersing factor coordinates pacemaker interactions in the *Drosophila* circadian system. J Neurosci 24:7951-7957.

Lipardi C and Paterson BM (2009) Identification of an RNA-dependent RNA polymerase in *Drosophila* involved in RNAi and transposon suppression. PNAS 106: 15645-15650.

Lipardi C, Wei Q, and Paterson BM (2001) RNAi as random degradative PCR: siRNA primers convert mRNA into dsRNA that are degraded to generate new siRNA. Cell 107:297-307.

Mertens I, Vandingenen A, Johnson EC, Shafer OT, Li W, Trigg JS, De Loof A, Schoofs L, and Taghert PH (2005) PDF receptor signaling in *Drosophila* contributes to both circadian and geotactic behaviors. Neuron 48:213-219.

Miyasako Y, Umezaki Y, and Tomioka K (2007) Separate sets of cerebral clock neurons are responsible for light and temperature entrainment of *Drosophila* circadian locomotor rhythms. J Biol Rhythms 22:115-126.

Moriyama Y, Sakamoto T, Karpova SG, Matsumoto A, Noji S, and Tomioka K (2008) RNA interference of the clock gene *period* disrupts circadian rhythms in the cricket *Gryllus bimaculatus*. J Biol Rhythms 23:308-318.

Moriyama Y, Sakamoto T, Matsumoto A, Noji S, and Tomioka K (2009) Functional analysis of the circadian clock gene *period* by RNA interference in nymphal crickets *Gryllus bimaculatus*. J Insect Physiol 55:396-400.

Okamoto A, Mori H, and Tomioka K (2001) The role of the optic lobe in circadian locomotor rhythm generation in the cricket, *Gryllus bimaculatus*, with special reference to PDH-immunoreactive neurons. J Insect Physiol 47:889-895.

Parisky KM, Agosto J, Pulver SR, Shang Y, Kuklin E, Hodge JJL, Kang K, Liu X, Garrity PA, Rosbash M, and Griffith LC (2008) PDF cells are a GABA-responsive wake-promoting component of the *Drosophila* sleep circuit. Neuron 60:672-682.

Park JH, Helfrich-Förster C, Lee G, Liu L, Rosbash M, and Hall JC (2000) Differential regulation of circadian pacemaker output by separate clock genes in *Drosophila*. PNAS 97:3608-3613.

Peng Y, Stoleru D, Levine JD, Hall JC, and Rosbash M (2003) *Drosophila* free-running rhythms require intercellular communication. PLoS Biol 1:32-40.

Petri B and Stengl M (1997) Pigment-dispersing hormone shifts the phase of the circadian pacemaker of the cockroach *Leucophaea maderae*. J Neurosci 17:4087-4093.

Reischig T and Stengl M (2003) Ectopic transplantation of the accessory medulla restores circadian locomotor rhythms in arrhythmic cockroaches (*Leucophaea maderae*). J Exp Biol 206:1877-1886.

Renn SCP, Park JH, Rosbash M, Hall JC, and Taghert PH (1999) A pdf neuropeptide gene mutation and ablation of PDF neurons each cause severe abnormalities of behavioral circadian rhythms in *Drosophila*. Cell 99:791-802.

Rieger D, Stanewsky R, and Helfrich-Förster C (2003) Cryptochrome, compound eyes, Hofbauer-Buchner eyelets, and ocelli play different roles in the entrainment and masking pathway of the locomotor activity rhythm in the fruit fly *Drosophila melanogaster*. J Biol Rhythms 18:377-391.

Rutledge RG and Cote C (2003) Mathematics of quantititative kinetic PCR and the application of standard curves. Nucleic Acids Res 31:e93.

Saifullah ASM and Tomioka K (2003) Pigment-dispersing factor sets the night state of the medulla bilateral neurons in the optic lobe of the cricket, *Gryllus bimaculatus*. J Insect Physiol 49:231-239.

Sakamoto T and Tomioka K (2007) Effects of unilateral compound-eye removal on the photoperiodic responses of nymphal development in the cricket *Modicogryllus siamensis*. Zool Sci 24:604-610.

Sauman I, Tsai T, Roca AL, and Reppert SM (1996) Period protein is necessary for circadian control of egg hatching behavior in the silkmoth *Antheraea pernyi*. Neuron 17:979-990.

Schneider N-L and Stengl M (2005) Pigment-dispersing factor and GABA synchronize cells of the isolated circadian clock of the cockroach *Leucophaea maderae*. J Neurosci 25:5138-5147.

Shafer OT, Kim DJ, Dunbar-Yaffe R, Nikolaev VO, Lohse MJ, and Taghert PH (2008) Widespread receptivity to neuropeptide PDF throughout the neuronal circadian clock network of *Drosophila* revealed by real-time Cyclic AMP imaging. Neuron 58:223-237.

Sheeba V, Fogle KJ, and Holmes TC (2010) Persistence of morning anticipation behavior and high amplitude morning startle response following functional loss of small ventral lateral neurons in *Drosophila*. PLoS ONE 5:e11628.

Sheeba V, Sharma VK, Gu H, Chou Y-T, O'Dowd DK, and Holmes TC (2008) Pigment dispersing factor-dependent and -independent circadian locomotor behavioral rhythms. J Neurosci 28:217-227.

Shiga S and Numata H (1997) Seasonal changes in the incidence of embryonic diapause in the band-legged ground cricket, *Dianemobius nigrofasciatus*. Zool Sci 14:1015-1018.

Sijen T, Fleenor J, Simmer F, Thijssen KL, Parrish S, Timmons L, Plasterk RHA, and Fire A (2001) On the role of RNA amplification in dsRNA-triggered gene silencing. Cell 107:465-476.

Singaravel M, Fujisawa Y, Hisada M, Saifullah A, and Tomioka K (2003) Phase shifts of the circadian locomotor rhythm induced by pigment-dispersing factor in the cricket *Gryllus bimaculatus*. Zool Sci 20:1347-1354.

Sokolove PG and Bushell WN (1978) The chi square periodogram: its utility for analysis of circadian rhythms. J Theoret Biol 72:131-160.

Stengl M (1995) Pigment-dispersing hormone-immunoreactive fibers persist in crickets which remain rhythmic after bilateral transection of the optic stalks. J Comp Physiol A 176:217-228.

Stengl M and Homberg U (1994) Pigment-dispersing hormone-immunoreactive neurons in the cockroach *Leucophaea maderae* share properties with circadian pacemaker neurons. J Comp Physiol A 175:203-213.

Taghert PH, Hewes RS, Park JH, O'Brien MA, Han M, and Peck ME (2001) Multiple amidated neuropeptides are required for normal circadian locomotor rhythms in *Drosophila*. J Neurosci 21:6673-6686.

Taghert PH and Shafer OT (2006) Mechanisms of clock output in the *Drosophila* circadian pacemaker system. J Biol Rhythms 21:445-457.

Tomioka K and Chiba Y (1982) Post-embryonic development of circadian rhythm in the cricket, *Gryllus bimaculatus*: a rhythm reversal. J Comp Physiol A 147:299-304.

Tomioka K, Miyasako Y, and Umezaki Y (2008) PDF as a coupling mediator between the light-entrainable and temperature-entrainable clocks in *Drosophila melanogaster*. Acta Biol Hung (Suppl) 59:149-155.

Tomioka K, Uwozumi K, and Matsumoto N (1997) Light cycles given during development affect freerunning period of circadian locomotor rhythm of *period* mutants in *Drosophila melanogaster*. J Insect Physiol 43:297-305.

Tomioka K, Wakatsuki T, Shimono K, and Chiba Y (1991) Circadian control of hatching in the cricket, *Gryllus bimaculatus*. J Insect Physiol 37:365-371.

Waddell B, Lewis RD, and Engelmann W (1990) Localization of the circadian pacemakers of *Hemideina thoracica* (Orthoptera; Stenopelmatidae). J Biol Rhythms 5: 131-139.

Yoshii T, Wülbeck C, Sehadova H, Veleri S, Bichler D, Stanewsky R, and Helfrich-Förster C (2009) The neuropeptide pigment-dispersing factor adjusts period and phase of *Drosophila's* clock. J Neurosci 29:2597-2610.

Zamore PD, Tuschl T, Sharp PA, and Bartel DP (2000) RNAi: double-stranded RNA directs the ATP-dependent cleavage of mRNA at 21 to 23 nucleotide intervals. Cell 101:25-33.